Geomorphic site assessment of Mesa Creek from 1937 to present at Sondermann Park, Colorado Springs, CO

El Paso County, Colorado

November 03, 2022

Prepared for:

Colorado Springs Parks, Recreation and Cultural Services
1401 Recreation Way
Colorado Springs, CO 80905

Prepared by:

Sarah Schanz, PhD
John Byers
Ren Carroll
Jack-Henry Kent
Fiona Swope

Colorado College Geology Department
14 E Cache la Poudre St
Colorado Springs, CO 80903

[page intentionally left blank]

Table of Contents

1. Introduction

1.1 Overview

Sondermann Park is located in Colorado Springs, CO (*Figure 1*). It is a city-managed park that is primarily used by walkers and bikers. The Beidleman Center at the trailhead hosts the Catamount Institute, a nonprofit that provides outdoor and ecology education outreach opportunities to pre-K and K-12 students. During this work, we observed many seniors using the trails, who spoke to the easy accessibility of the wide, graded paths and situation within neighborhoods, including Mesa, Mesa Springs, and Kissing Camels neighborhoods. The throughgoing Mesa-Palmer trail connects the Westside and Central Colorado Springs bike trails to Mesa Road and access to Garden of the Gods.

In 2022, extension of Centennial Boulevard from Van Buren Street to the Fontanero Interchange impinged on the northeast corner of Sondermann Park and leveled grasslands that had been informally connected to the park through single-track trails.

1.2 Scope of work

In summer 2021, members of the Colorado Springs Department of Parks, Recreation & Cultural Service reached out to Professor Sarah Schanz about potential restoration of Mesa Creek and riparian areas through Sondermann Park. To understand the geomorphic background that influences erosion, stability, and complexity of Mesa Creek, Professor Schanz and the GY400: Collaborative Research Seminar class compiled historic data from 1937 to present and investigated modern channel and bed characteristics.

Specific tasks and objectives of this work are as follows:

- Assess historic changes to the channel, particularly vegetation density
- Quantify modern channel form and process
- Compare modern process to historic through sedimentary archives
- Analyze spatial patterns of channel complexity and potential biodiversity

Through all of these objectives, the influence of vegetation on channel form, process, and complexity is a primary focus.

This report synthesizes information collected and analyzed from February 21 to April 20, 2022 and is organized in the following sections:

- 3.1 Channel classification
- 3.2 Vegetation and ecology
- 3.3 Sediment size in modern and historic deposits
- 3.4 Channel complexity
- 3.5 Hydrologic modeling

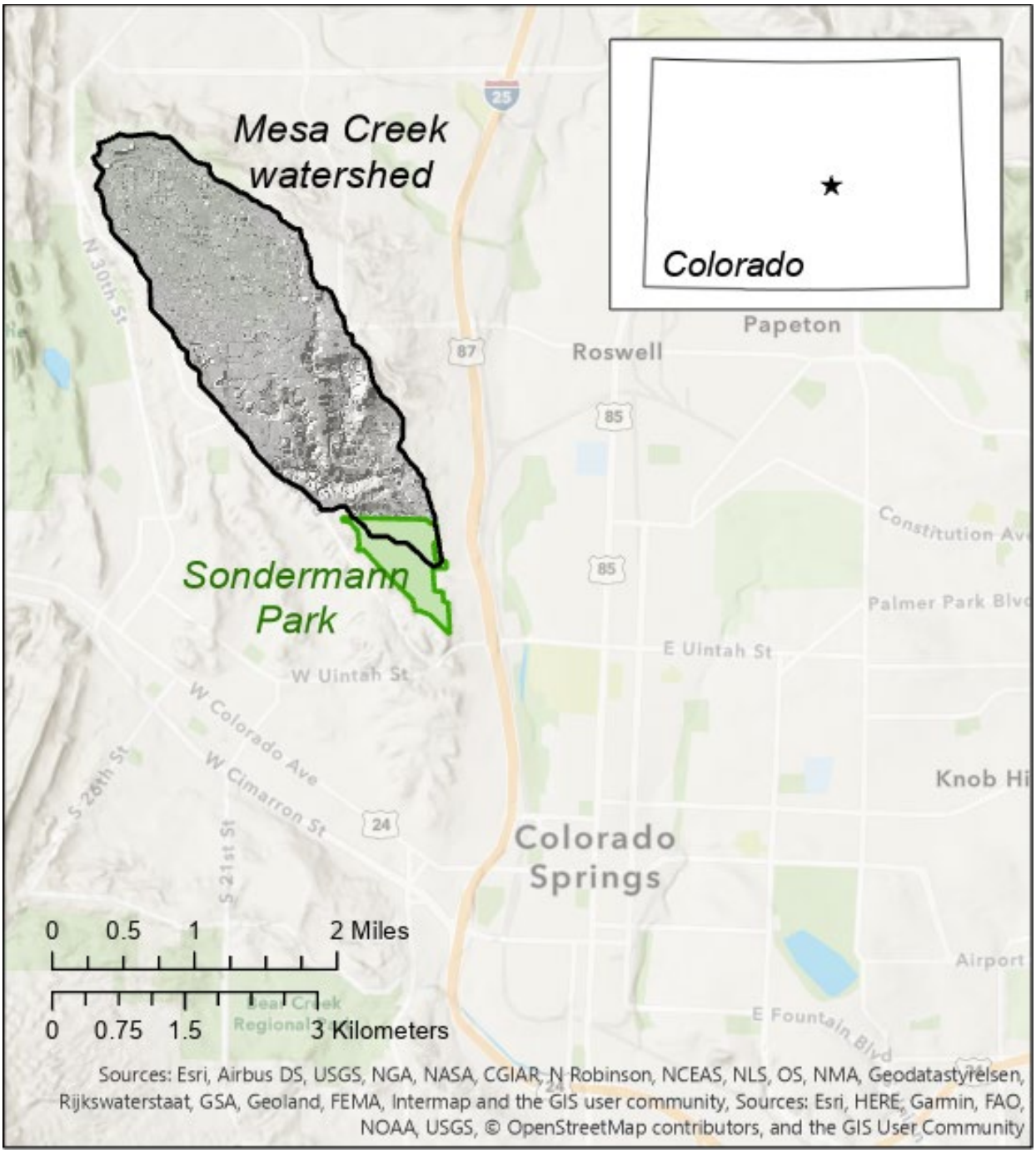

Figure 1. Location of Mesa Creek and Sondermann Park within the Colorado Springs urban area. Inset shows the location of Colorado Springs within the state of Colorado.

1.3 Background on urban streams

The impact of urban development on rivers and streams has been an increasing topic of study in the past 50 years, reflecting global population and urban area growth (Chin, 2006). Land surface modifications during urbanization impose fundamental changes in channel morphology, hydrology, sediment production and yield, run-off processes, and ecology (Booth and Fischenich, 2015; Chin, 2006). Collectively, the typical urban stream physical and ecological response to urbanization is termed the urban stream syndrome (Booth et al., 2016) and is generally caused by increased flashiness of storm events and increased sediment loads. Global analyses of sediment loads indicate 2-10 times increase in sediment yields immediately post-urbanization with up to 20-80 times increase during storms (Chin, 2006). Symptoms of the urban stream syndrome include heavy erosion and incised, straightened channels (Chin, 2006); greater frequency and magnitude of high flow events (Booth and Fischenich, 2015); and degraded water quality and biota health (Van Meter et al., 2016). These impacts to stream characteristics manifest over a temporal scale first described by Wolman in 1967 in which streams evolve from a pre-development stage over the course of active development before stabilizing at a quasi-equilibrium state in their new urbanized landscape (Chin, 2006). Urban development causes a channel response in under a year, yet it can take decades to potentially centuries for streams to reach a new quasi-equilibrium state (Booth et al., 2016).

However, the majority of work on urban streams focuses on regions in temperate climates and only a handful of studies address channel response in arid to semi-arid regions. Streams in semi-arid climates often have highly variable and less predictable responses to urbanization due to sparse vegetation cover, naturally flashy flows, and variable bed mobility (Chin, 2006). For instance, in southern California, urbanized semi-arid streams can switch between single and multi-thread quasi-equilibrium in response to urbanization and can show up to 1000% channel enlargement in <10 years (Hawley et al., 2012). Timescales of response can be variable, as high flows are relatively fewer and far between than in temperate rivers. Increased base flows from irrigation narrow and channelize semi-arid streams to a larger degree than their temperature counterparts, and result in reduced bed and bank mobility (Hawley et al., 2012).

Mesa Creek presents an opportunity to further knowledge on semi-arid urban streams. Booth et al. (2016) emphasized the need for nuanced, site specific interpretations of urban streams before sustainable progress toward remediation can be made. Beyond the fact that semi-arid stream responses to urbanization are poorly understood, Mesa Creek is also actively undergoing increased urbanization in its watershed through the extension of Centennial Boulevard. Further, Mesa Creek's urbanization process is atypical; urbanization began in the headwaters and spread downstream. Studying Mesa Creek will provide insight into the range of morphological changes caused by urbanization, and will provide a baseline for future site work post-Centennial Boulevard construction.

2. Mesa Creek, Colorado Springs

2.1 Geology and geomorphology

The study site encompasses the downstream portion of Mesa Creek within the Sondermann Park extent (*Figure 2*), and lies within the 2.2 square mile Mesa Creek watershed. The watershed extends north to just south of Garden of the Gods Road, west to Mesa Road, east to Centennial Boulevard, and curves to meet

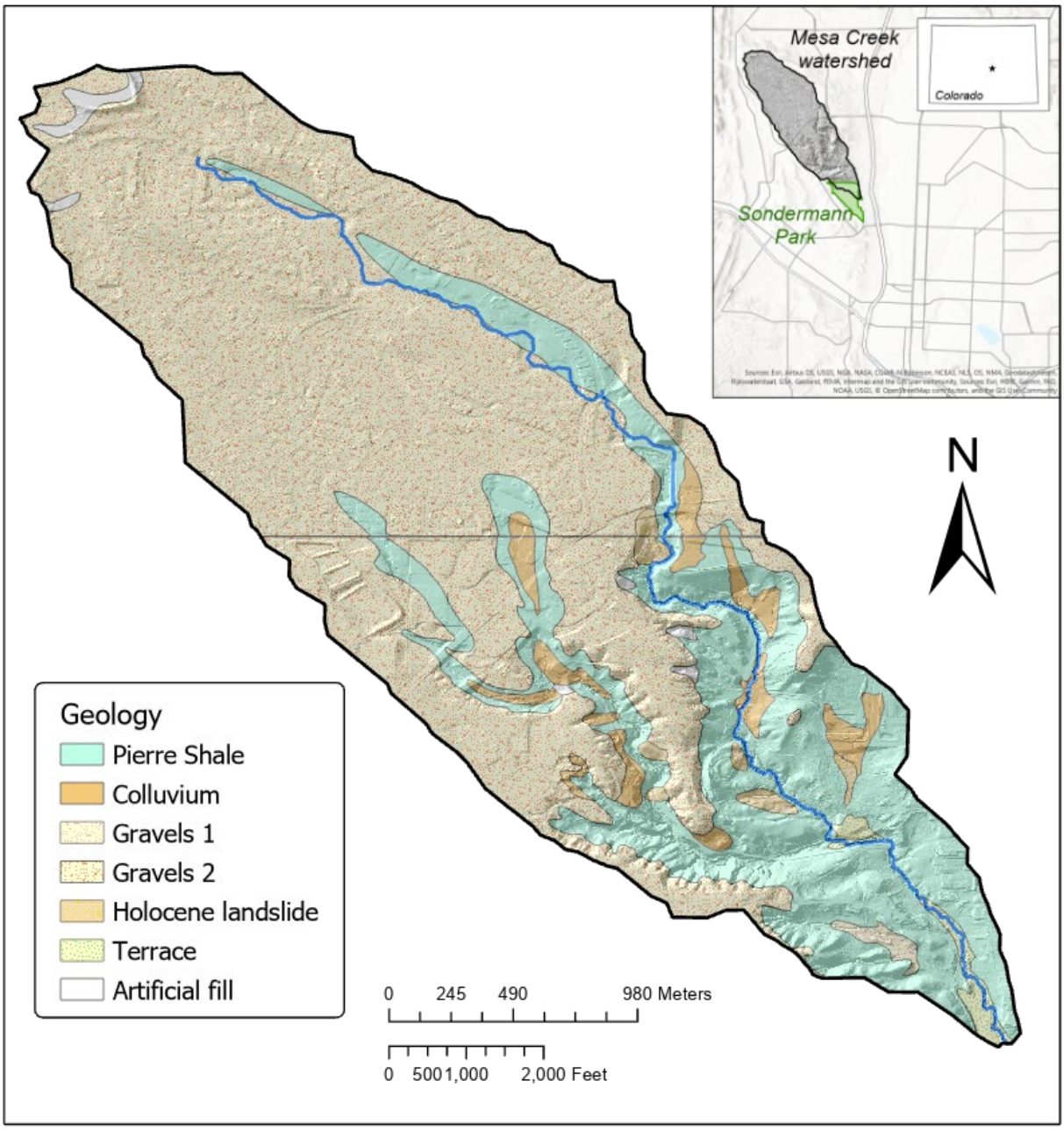

Figure 2. Geologic map of Mesa Creek watershed.

Monument Creek at Caramillo Street. The stream begins at 6600 ft above sea level and falls to 6017 ft at the confluence with Monument Creek.

Mesa Creek is underlain by the Cretaceous Pierre Shale (*Figure 2*). The Pierre Shale ranges in thickness from 5,000 feet under Colorado Springs, CO, to more than 8,000 feet near Boulder, CO (Scott and Cobban, 1965). The shale formed in an upper Cretaceous shallow sea and alternates between large beds of shale and sandstone with smaller interbeds composed of shale, limestone, and sandstone. In the region under Mesa Creek, the Pierre Shale is predominantly a black shale with occasional cobble-sized concretions found at the northern end of Sondermann Park. The bedded shales dip gently to the east.

The headwaters of Mesa Creek originate on a mesa composed of gravel clasts that unconformably overlie the Pierre Shale as a strath terrace. The gravels are locally referred to as the Mesa Gravels and comprise sand to cobble clasts of mostly Pikes Peak Granite. The age of the Mesa Gravels is not well constrained, but is Early to Middle Pleistocene (Peters et al., 2018).

As the stream descends from the Mesa Gravels, the landscape becomes heavily gullied with historic landslide complexes and potential for debris flow activity (White and Wait, 2003). The western valley wall within Sondermann Park is susceptible to landslides, though no known landslides have been mapped within the Park boundaries.

Soils in the watershed reflect the underlying geology (*Figure 3*). The mesa headwaters underlain by the Mesa Gravels contain a well-drained sandy loam soil called Ascalon which covers 49% of the watershed (Web Soil Survey). The landslide-prone slopes coming off the Mesa Gravels are characterized by the Chaseville-Midway soil complex of gravelly sandy loam to clay loams. This soil complex tends to be excessively drained to well-drained. At the downstream end, including the Sondermann Park region, soils are the well-drained stony clay and clay loams of the Razor-Midway complex. The Razor-Midway complex forms from weathered shale, and reflects soil growth through weathering of underlying bedrock rather than soil accumulation through depositional processes.

2.2 Climate

The climate at Mesa Creek is characterized as semi-arid with dry and cold winters and hot summers. In the Koppen-Geiger classification, the region has a warm-summer humid continental climate (Peel et al., 2007). The mean annual temperature is 46.5 °F and mean annual precipitation is 20.9 inches (https://en.climate-data.org/). Precipitation falls mostly in the summer as short-lived and spatially discrete convection storms. The 100-year 6-hour precipitation event is 4.6 inches (U.S. Geological Survey, 2016); most precipitation events are much less. Snowfall during winter months lasts for 1 to 2 days before melting, though accumulation under shade can persist for weeks.

Precipitation is spatially variable, making it hard to correlate events between weather stations. The closest weather station to the study area is the Camp Creek station at Garden of the Gods, 2.21 miles northwest of Sondermann Park. This station has precipitation records from 2007 to present that indicate 0.18 inches of average daily precipitation when precipitation occurs, and annual peak events of 1 to 5.76 inches/day.

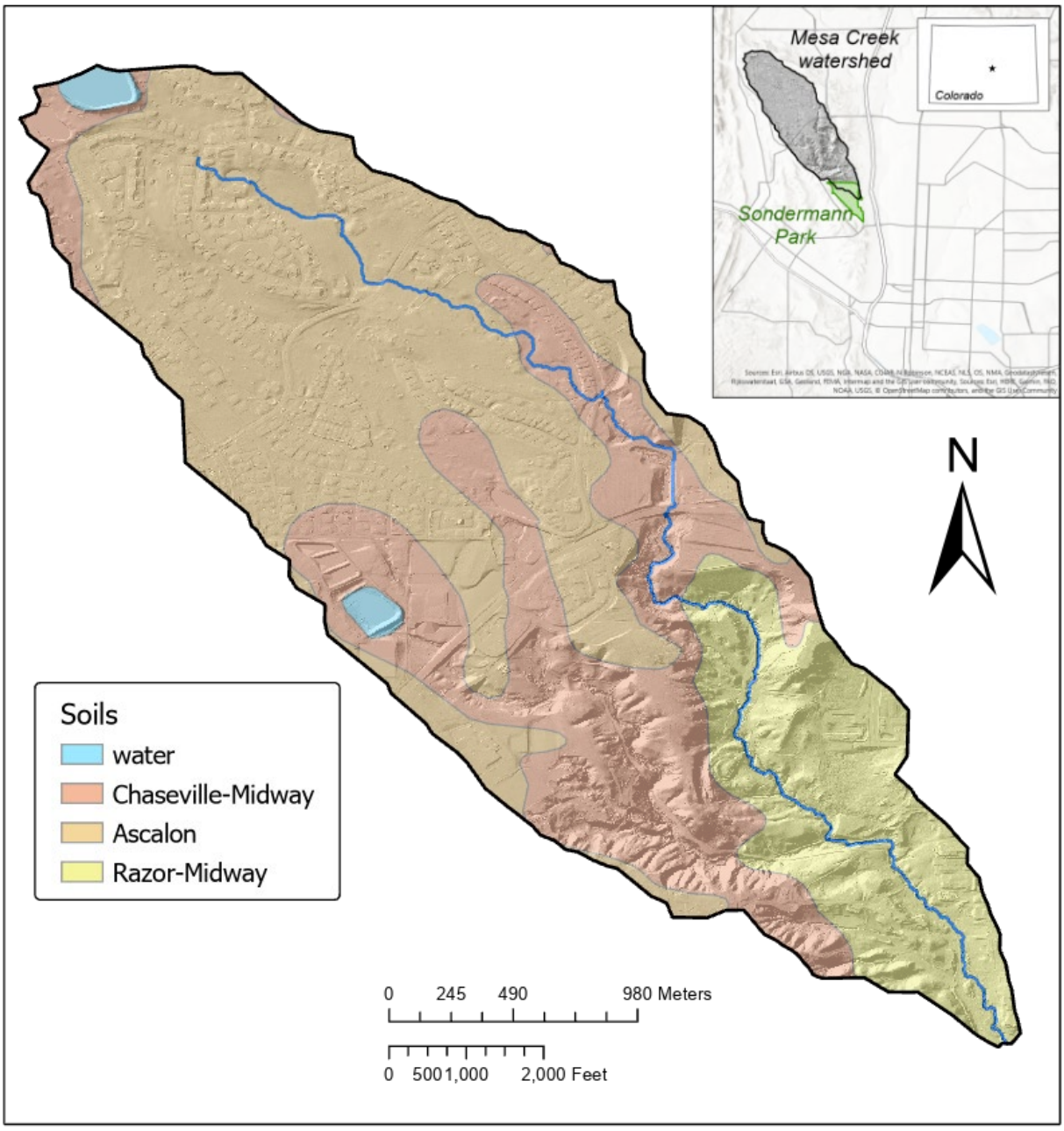

Figure 3. Soils map of Mesa Creek watershed.

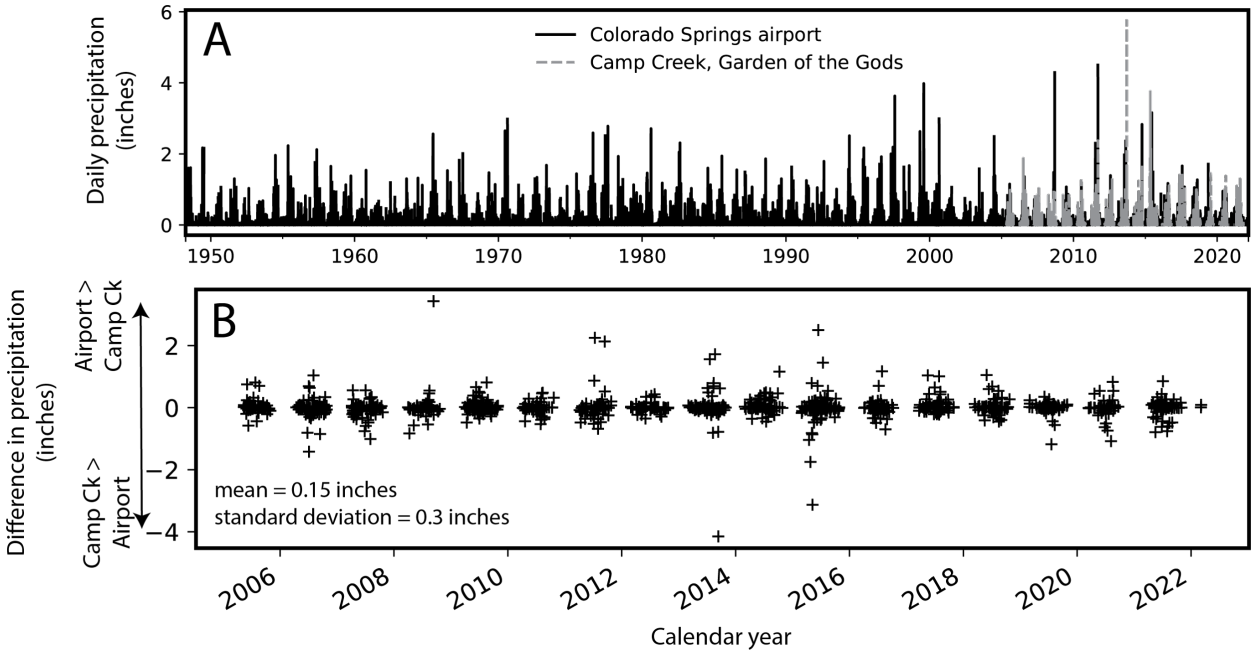

Figure 4. Comparison of precipitation records at the Colorado Springs airport and Camp Creek weather stations. A) Daily precipitation over the full record from 1948 to present and 2007 to present. B) Difference in daily precipitation for days when either Camp Creek or Colorado Springs airport records non-zero accumulation.

A longer-term record since 1948 is available from a weather station at Colorado Springs Airport, 8.3 miles southeast of Sondermann Park. However, comparison to the Camp Creek station shows that storm events that hit the Airport station differ in rainfall totals from Camp Creek (*Figure 4*). On average, when precipitation occurs at either Camp Creek or the Airport, the two stations record differences of 0.15 ± 0.3 inches on average. Considering that average precipitation events at Camp Creek are 0.18 inches/day, the two stations show considerable difference in precipitation patterns. Thus, a long-term analysis of precipitation at Mesa Creek is not possible, and this study cannot analyze large storm events pre-2007.

2.3 Land cover and use

Mesa Creek is in the Central Prairie Shortgrass Ecoregion, which is a temperate grassland. Hillsides are covered in grasses with some low shrubs clustered in gullies and waterways. Close to surface water, shrub density increases and reeds are common. Cottonwoods and other deciduous trees grow near the channel of Mesa Creek with isolated pine and fir stands at Sondermann Park. These latter stands were likely planted in the 1930s, based on aerial photos. Aquatic species abundance and diversity are not well described across the ecoregion, though trees show signs of active beavers and one minnow and one aquatic snail shell were observed in our study.

As the Colorado Springs urban area grew, urbanization in the Mesa Creek watershed increased. Development was initially limited to a few houses in the southern edge of the watershed and to the El Paso Canal. The canal was constructed in 1871 and diverted water from Fountain Creek near 30th Street, carried it 6.5 miles, and delivered water to the Roswell neighborhood and eventually to Boulder Park (https://www.cspm.org/). The canal was shut down in 1956, but remnants of the canal bridge across Mesa

Creek can still be seen approximately 250 feet upstream of the upstream foot bridge in Sondermann Park, and its path can be traced in the western hillside.

During the first half of the 20th century, residential growth into the Mesa Creek watershed was slow. However, in the 1950s, growth along the mesa top increased with residential houses and construction of the Kissing Camels Golf Course and Resort (*Figure 5*). The golf course was laid down over the headwater gullies of Mesa Creek, and resulted in year-round irrigation and water delivery to the stream. This has increased base flow, and we explore implications of increased base flow on vegetation and channel stability in sections 3.1, 3.2, and 3.5.

After the golf course, development continued as Mesa Road and Fillmore Street were paved and residential areas built. Commercial construction along Fillmore Street increased impervious surfaces, especially as Fillmore and Centennial were expanded to four lane roads. In the mid to late 20th century, a landfill just north of Sondermann Park was in operation. Although it closed decades ago, tires and trash are often excavated during heavy rains (KRDO, 2019) and green leachate has been observed by residents (city-data, 2019). The 2018 extension of Centennial Boulevard and subsequent 2022 extension included plans to clean up the old landfill and dump sites.

The most recent development in the Mesa Creek watershed is the Centennial Boulevard extension, which is planned to be a four-lane road with sidewalks and bike lanes. The 2018 extension slightly increased impervious surfaces along the eastern edge of the watershed, but the 2022 construction significantly impedes into the watershed. Construction plans include a culvert and runoff collection system that diverts runoff from the road to a retention pond, which can hold a 100-year storm event and release the runoff into Mesa Creek over a 72-hour period. The road is outside the 100-year floodplain of Mesa Creek, although the riparian area along Mesa Creek was removed in the March 2022 construction. This implies some structures may eventually impede on the floodplain.

Post-construction, MVS Development LLC will build a 400-home complex on the north edge of Sondermann Park, just northeast of where Mesa Creek splits into two major tributaries. This will likely increase impervious surfaces and runoff patterns, but detailed plans were not accessible to this study.

These ongoing and planned construction projects have the potential to alter the runoff and sediment characteristics of Mesa Creek and cause aggradation within the urban stream syndrome. However, as previously mentioned, few studies quantify the urban stream syndrome response for semi-arid urban streams, and the unique spatial distribution of urbanization—in which impervious surface concentrations are higher at the headwaters and lowest downstream—around Mesa Creek further sets this stream apart. In this study, we approach the stream from a geomorphology perspective to understand: current channel morphology, historic changes to vegetation and ecology, sediment size distributions now and in the past, channel complexity, and hydraulic flow patterns. By examining these variables, this study seeks to elucidate the role that altered base flow due to irrigation, increased impervious surfaces, and vegetation changes have on the state of Mesa Creek.

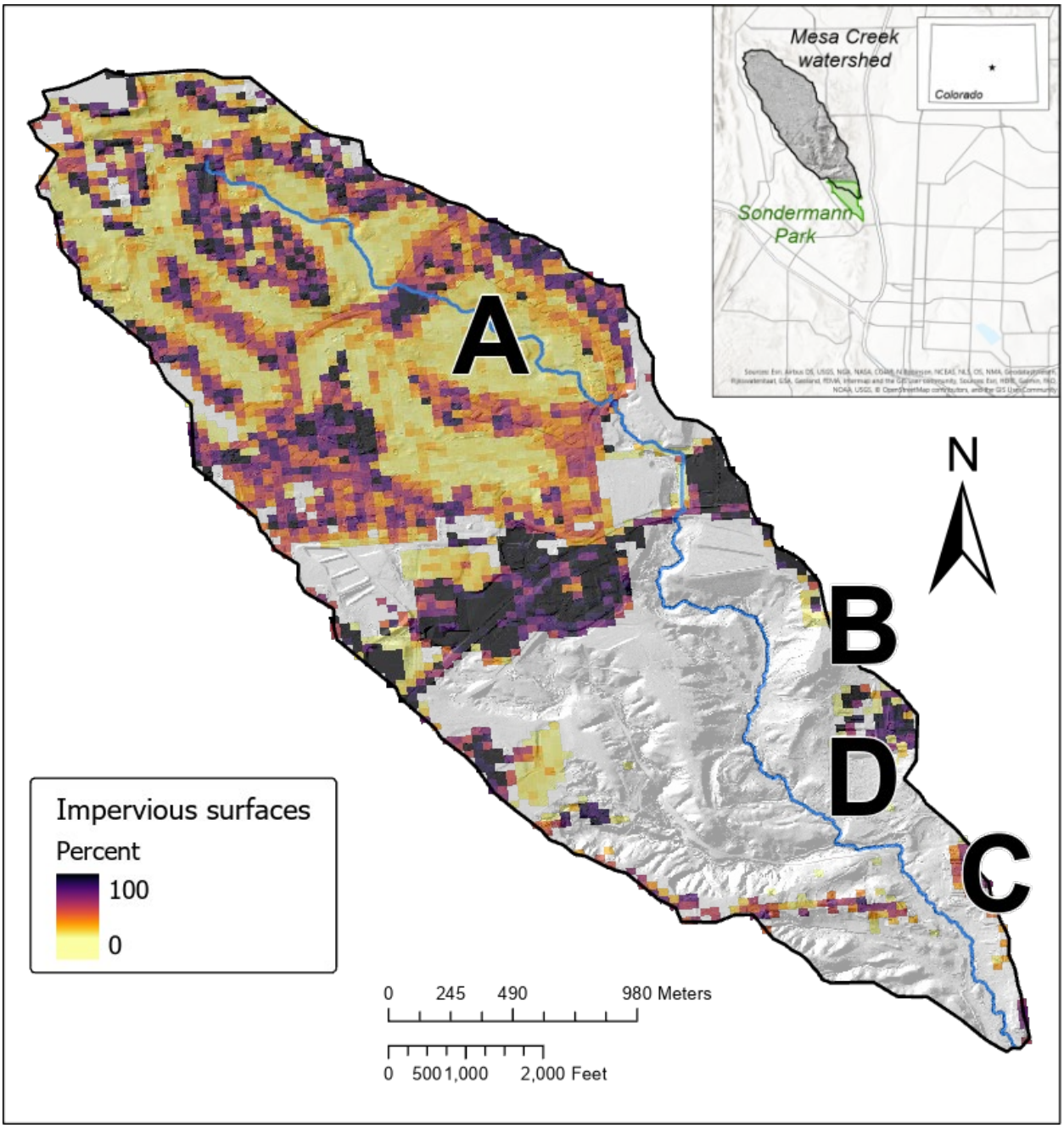

Figure 5. Impervious surface map showing percent impervious surfaces in 2019. Areas of interest are noted: A) Kissing Camels Golf Course, B) Centennial Boulevard 2018 extension, C) Centennial Boulevard 2022 extension, and D) proposed MVS Development LLC housing complex.

3. Methods and Results

3.1 Channel classification

3.1.1 Methods

Mesa Creek through Sondermann Park was classified by Rosgen channel type (Rosgen, 1994) based on the degree of entrenchment, channel slope, grain size, number of channels, and sinuosity (*Figure 6*). Each reach was at least 20 channel widths long. Initial reach classifications were done in the field, but classifications were revised the next day to incorporate quantitative entrenchment values and keep internal consistency between similar reaches.

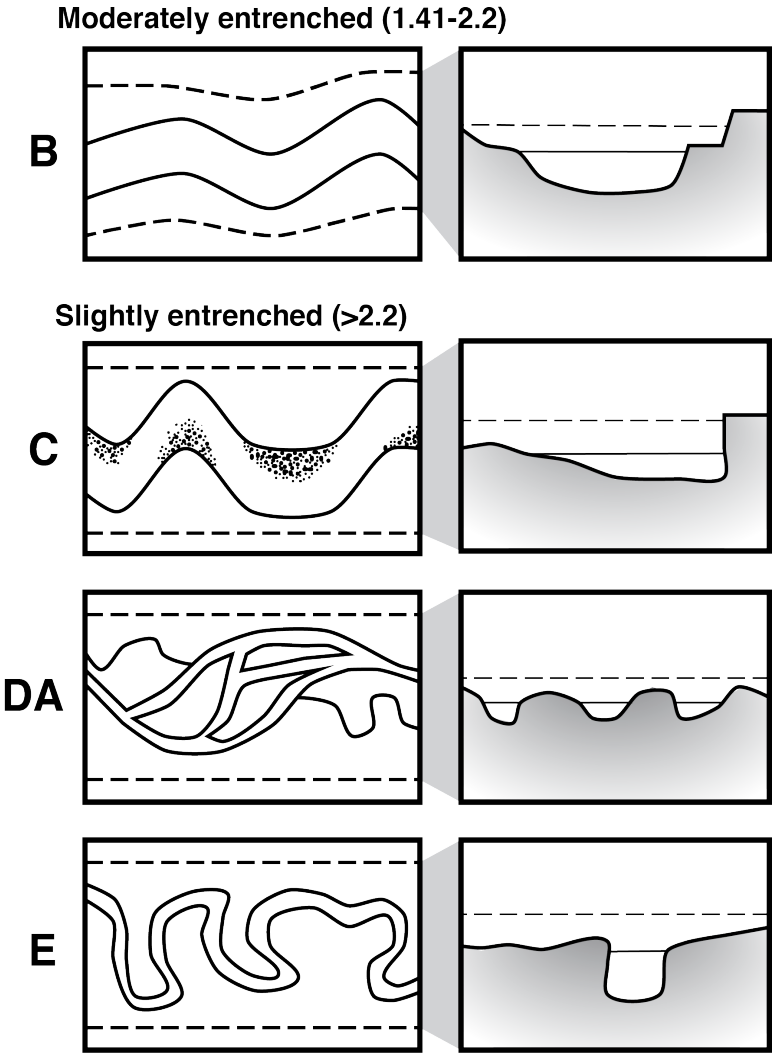

Figure 6. Rosgen reaches used in this study, modified from Rosgen (1994). Left panels show planviews while right panels show a cross section. Dashed lines indicate the flood-prone width and solid lines are the bankfull width. Entrenchment is the ratio between flood-prone and bankfull widths.

3.1.2 Results

The Rosgen classification resulted in 11 distinct channel reaches. Channel sinuosity was lower in Mesa Creek than the template Rosgen classifications (*Table 1*); due to the small stream size, the Rosgen classification that best fit each reach was used. Because of this, we caution that Rosgen classifications throughout Mesa Creek should be used to distinguish reaches but should not be used to infer geomorphic processes a la Rosgen (1994)'s Table 3.

Of the 11 distinct reaches, four main channel types of B, C, DA, and E were observed with secondary variations in estimated grain size and slope (*Figure 7*). C, or single thread channels with slight entrenchment, were the most common channel type in the study area, comprising just over 50% of the channel length (*Figure 8*). The longest single extent is channel type DA, or multi-threaded channels with high sinuosity and slight entrenchment. The two upstream DA reaches were 587 and 577 feet long, while the longest individual C type reach was 442 feet long (*Table 1*).

The slope of each reach, extracted from 2 ft lidar obtained from the Colorado State Governor's Office of Information Technology, was relatively similar for channel types C, DA, and E. Slope averaged 0.013 ft/ft between those three channel types. The exception is reach C6c-, which was noted in the field to have a lower slope and was confirmed by GIS to have a slope of 0.0044 ft/ft. Channel type B, which is noted as having moderate entrenchment compared to the other channel types, had a greater slope of 0.0264, twice that of the other reaches. Notably, this is in the middle of the study area (*Figure 7*), and so likely represents a knickzone–an oversteepened stream segment–rather than an equilibrium slope. Graded or equilibrium channels will have higher slopes in the upstream reaches and gradually decrease slope downstream.

Table 1. Rosgen classification reaches for Mesa Creek

ID	Rosgen type	length (ft)	sinuosity (ft/ft)	slope (ft/ft)
1	C4	235.67	1.75	0.0091
2	C6c-	264.34	1.02	0.0044
3	DA6	577.50	1.13	0.0099
4	C6	152.49	1.01	0.0064
5	DA6	587.07	1.08	0.0131
6	C4	442.60	1.09	0.0196
7	DA5	193.21	1.09	0.015
8	B5c	236.54	1.06	0.0264
9	E5	196.68	1.33	0.0188
10	C4	295.61	1.31	0.0092
11	C5	410.24	1.06	0.0163

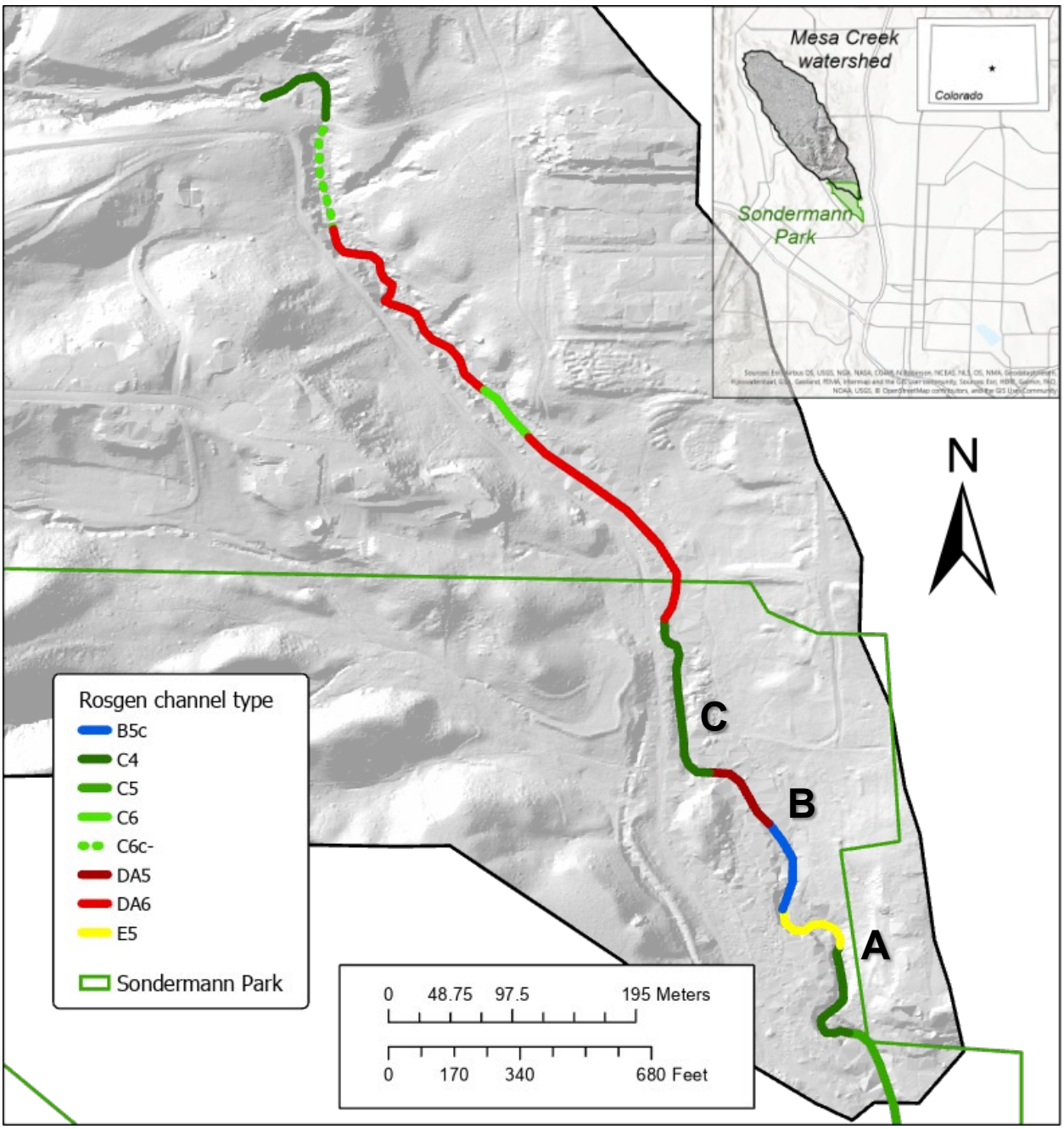

Figure 7. Rosgen reach classifications along Mesa Creek in the focused study area. Areas of interest that are discussed in the text are noted with letters.

Knickzones and knickpoints–discrete locations of over steepened slope–were also noted as dividing Rosgen reaches. On the downstream end of the E5 reach at the transition to C4 (location A in *Figure 7*), a small (~2 ft) knickpoint is created by a cottonwood root mass. Greater entrenchment downstream of the knickpoint suggested it had migrated upstream before being temporarily caught on the more resistant tree roots. Similarly, a knickpoint created by roots and small to large woody debris defined the transition from the multithreaded DA to the entrenched B5c zone (location B in *Figure 7*). Downstream of the knickpoint, the channel is entrenched and has a greater slope (0.0264) due the recent upstream passage of the knickpoint. Upstream, the accumulation of woody debris ponded the channel and diverted it into multiple channels, forcing the DA channel type and resulting in occasional flooding of the upstream picnic area.

Other observations support a strong vegetation control on the formation of Rosgen reaches. Upstream of the second footbridge in a C4 channel reach, a small woody debris dam has ponded the channel and forces the overflow onto the floodplain (location C in *Figure 7*). During our visits from 3/1 to 3/2/2022, the overflow was dispersed across the floodplain and flowed slowly to the main channel. However, on our 3/8/2022 visit, recent snowmelt augmented the streamflow, increasing overflow and channelizing it into a short DA reach. While this was below our threshold of 20 channel widths to map, it was a good demonstration of how easily the channel can transition between the DA and C reaches with the aid of even small woody debris.

3.1.3 Summary

Mesa Creek through the study area is majority a single thread, slightly entrenched channel but frequently alternates to a multi-threaded slightly entrenched channel. In two locations, the channel deviates from these: a short section with higher sinuosity but similar entrenchment, and a section just upstream of that where knickpoint incision has created a single thread, moderately entrenched channel. The transition between channel types is often modulated by vegetation; roots can temporarily halt knickpoint passage and thus form a boundary between moderate and slight entrenchment, and woody debris accumulations can force upstream ponding and diversion into a multi-threaded channel.

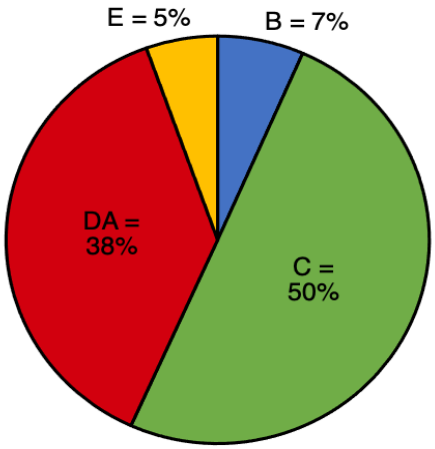

Figure 8. Percent of Mesa Creek in each Rosgen Classification, by length.

3.2 Vegetation and Ecology

3.2.1 Historical change

3.2.1.1 Methods

Historical analysis of vegetation cover in Sondermann Park was conducted using aerial photograph analysis. Through the US Geological Survey and CU Boulder, we identified, downloaded, and georeferenced aerial photos from 1937, 1947, 1953, 1960, 1969, 1975, 1983, 1991, 1993, 1999, 2002, 2008, 2011, 2013, 2015, 2017, and 2019 that cover Mesa Creek and Sondermann Park. We mapped the density of vegetation cover for seven aerial photographs in 1937, 1947, 1953, 1960, 1969, 1975, and 2002 over three study zones (*Figure 9*). These zones were selected from different reaches of the creek that represent varying degrees of urban influence. Zone 1 is located along an upper reach of Mesa Creek that has been reservoir fed since 1937 and underwent gradual urban development between 1969 and 2002. Zone 2 is also located on an upper reach of Mesa Creek. This zone captures vegetation changes along a reach that did not experience significant urbanization until 1993 but experienced a marked increase in base flow after 1960 due to the construction and irrigation of the Kissing Camels golf course. Zone 3 is located downstream of the other zones in order to capture general trends in watershed vegetation cover; it is the only zone located within our focused study area. The study zones were created in ArcGIS as polygons that buffer 82 feet (25 m) on either side of the channel centerline. Each reach extends for ~980 feet (~300 m). The visible and significant vegetation within these areas was mapped at 1:1000 scale in ArcGIS Pro. In the aerial imagery, trees and bushes appear as darker shapes that often line channels and gullies (*Figure 10*). Vegetation cover was delineated as polygons, and the sum total area of these polygons was used to calculate the percent vegetation cover, or vegetation density, for each zone at each image year.

3.2.1.2 Results

Early photographs show a grassland watershed with urbanization near the mouth, close to the present-day Biedlemann Center. The upstream mesas are mostly empty with a few roads, and channels are associated with low brush cover (*Figure 10*). Within modern Sondermann Park, pine tree saplings start to obscure the channel; however, Mesa Creek is clearly seen in its southward flowing stretch as a broad, unvegetated channel in 1937 and 1947. Vegetation begins to stabilize in 1953, and continues until the channel is covered by dense vegetation by 1969 (*Figure 10*). The 1937-1947 channel appears to be a braided channel with high mobility and a dynamic channel bed. Over time, this mobility is lost, as indicated by the stable vegetation.

Whether vegetation led to mobility loss or whether mobility loss was caused by another factor is unclear. Quantification of vegetation density corroborates the observational findings. The percent vegetation cover of the Mesa Creek watershed increased between 1937 and 2002 for all three mapped zones (*Figure 11*). The average percent cover across all zones rose from ~14% (1937) to ~39% (2002). Vegetation cover did not linearly increase in Zones 1 and 3. Both zones saw vegetation increase between 1937 and 1947 before decreasing again in 1953 to 10% and 12% respectively. Vegetation cover then increased slightly in Zone 1 but remained below 15% until 1969. In the same time period, Zone 3 experienced a rapid increase in vegetation, more than doubling between 1953 and 1969. Interestingly, between 1969 and 1975, vegetation cover decreased in the downstream Zone 3 while increasing dramatically in Zone 1. The two zones then experienced a gradual increase in vegetation cover through 2002. The increasing vegetation cover with time in Zones 1 and 3 is statistically significant with p-values of 0.07 and 0.001, respectively.

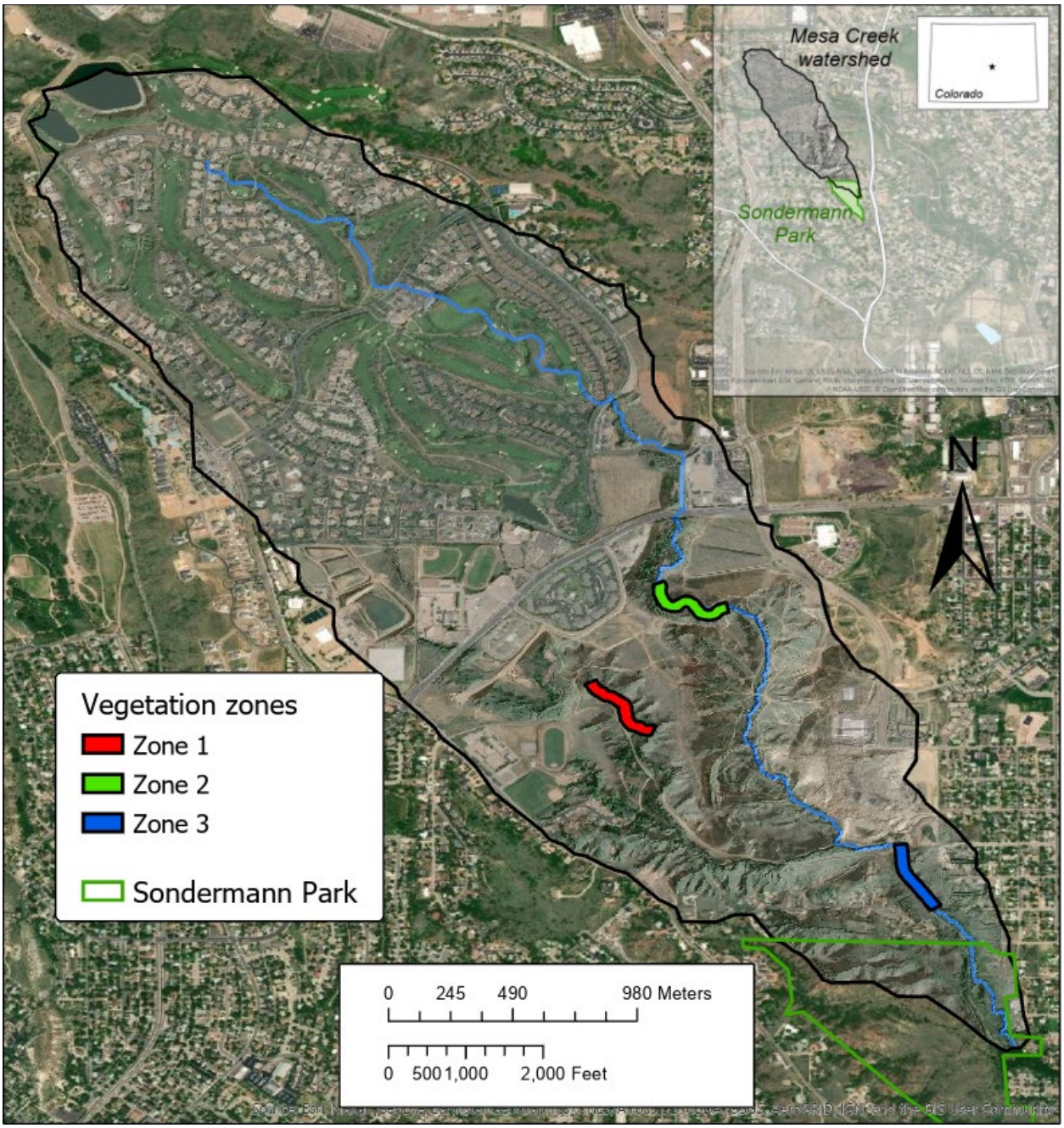

Figure 9. Location of vegetation density zones in Mesa Creek watershed.

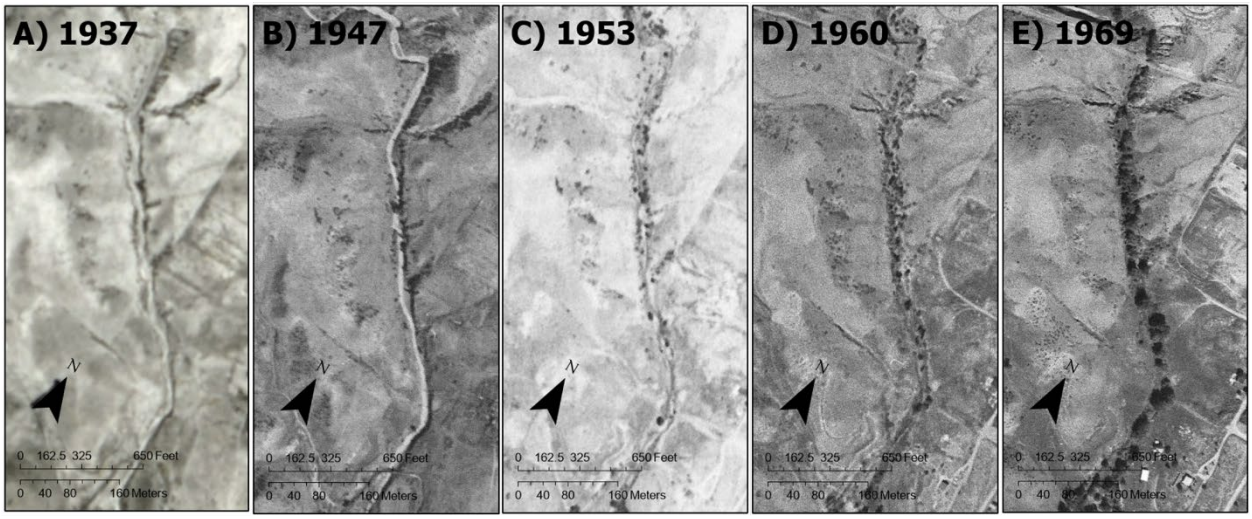

Figure 10. Mid 20th century channel changes recorded in the aerial photographs of Mesa Creek just north of the current Sondermann Park boundary in Zone 3.

The trend in vegetation cover in Zone 2 was less variable than in the other two studied zones. Percent vegetation cover increased every year with the greatest increase observed between 1947 and 1953, corresponding with the construction of the Kissing Camels golf course. With the exception of 1947, Zone 2 had greater vegetation cover than the other two zones and had above average vegetation in every aerial photograph analyzed. The increasing vegetation cover trend observed in Zone 2 is very significant according to the p-value of 0.0001.

Zone 2 did not experience significant impervious surface growth and upstream construction until the mid to late 1980s, yet had steady vegetation densification from 1950 onward. This phenomenon is potentially explained by the construction and irrigation of the Kissing Camels golf course. While this did not increase impervious surfaces, and thus flashiness, of the contributing watershed, it did provide a steady base flow. Hawley et al. (2012), working in semi-arid streams of Southern California, noted a similar trend of vegetation densification due to urban water inputs. Although Zones 1 and 3 are also downstream of the

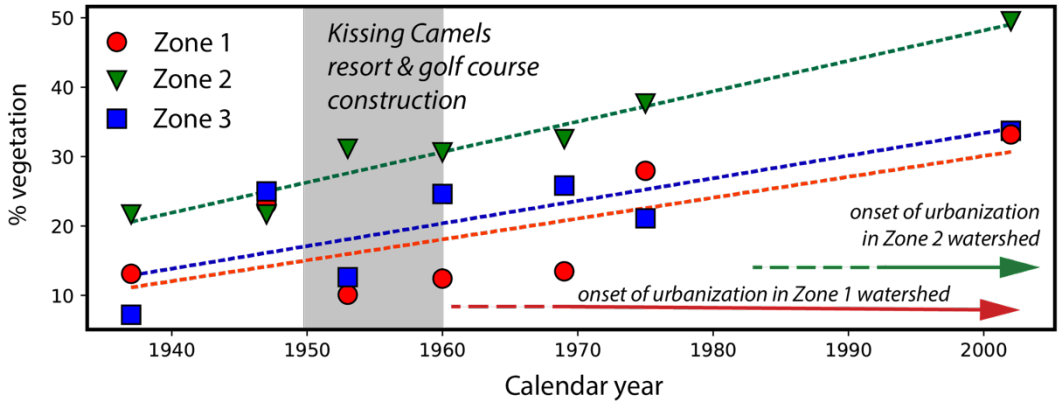

Figure 11. Vegetation density over time for three vegetation zones. Significant urbanization events noted.

Kissing Camels irrigation, both experienced urbanization and construction from 1960 onwards. These two zones are more likely to experience disturbance due to sedimentation resulting from construction, which can temporarily aggrade or cause increased channel mobility, leading to partial de-vegetation. Overall, despite variations in percent vegetation trends in Zones 1 and 3, the Mesa Creek watershed experienced a growth in and densification of vegetation between 1937 and 2002.

3.2.2 Present Conditions

In addition to the historical extent of vegetation, qualitative observations of vegetation and ecology were gathered during a week of field work in Sondermann Park conducted in early March, 2022. Observations focused on overall vegetation patterns, riparian zone health, vegetative control on stream banks and channels, and ecological indicators. These notes provide a useful, if limited, look into the biological function and characteristics of Sondermann Park in its present condition.

The character and type of vegetation cover varied spatially across the study area. In the most upstream reach of our focused study area (*Figure 7*), medium sized trees and bushes interspersed with grasses grow on sandy floodplains. Downstream of this and within the upstream-most DA reach, vegetation consisted more of bushes and reeds, with infrequent large woody growth. Snags of trees 1.6 to 3 feet in diameter rose above the shrubs. Basal trunks were buried by the modern floodplain, and trees appears to have grown when water levels were at the elevation of the current channel bottom, indicating the modern channel aggraded at least 1.3 feet (0.4 meters). At the beginning of the second DA reach (*Figure 7*), the vegetated floodplain began to be dominated by stands of large cottonwood trees with sparse underbrush. Ponding of the stream had elevated water levels, though not to a degree that tree health was negatively impacted (*Figure 12A*). The growth of large trees remained limited to the floodplain. Along the most downstream reaches within the Sondermann Park boundary, the trees thinned and spread onto terraces while tall grass and bushes stabilized stream banks. Pine trees became common in this section. On the most heavily foot trafficked sections of the park (including bridge crossings and picnic area) the stream banks were bare.

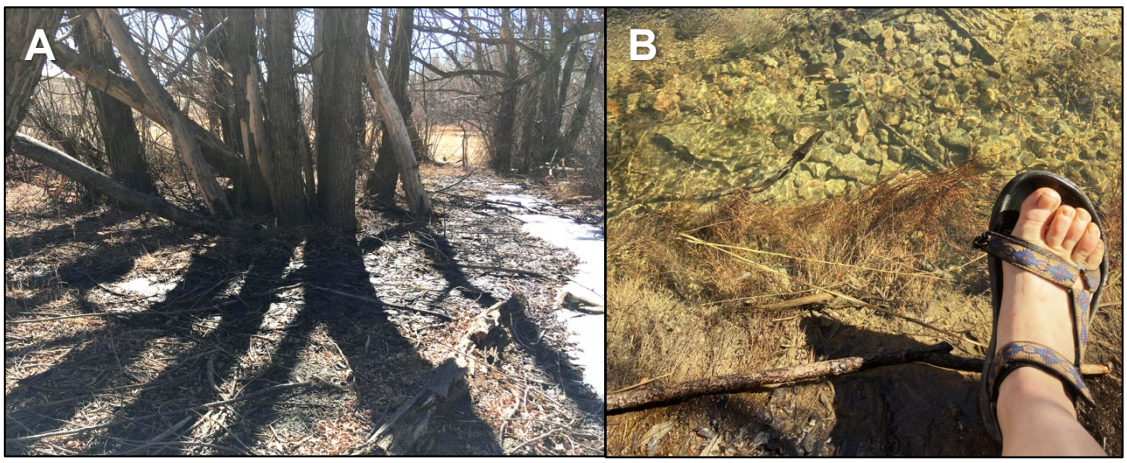

Figure 12. Vegetation observations included A) a flooded stream section drowning cottonwoods and other plants, and B) root mat control on stream bank strength and morphology.

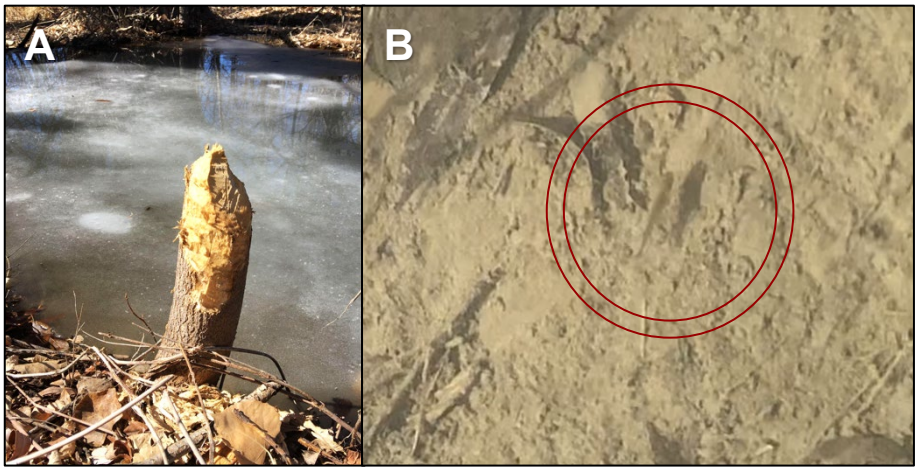

Figure 13. Ecologic observations include A) a recently beaver cut tree near a debris jam and B) small fish in Mesa Creek, circled in red.

Dense root mats are a strong control on stream banks and channelization along some portions of Mesa Creek. Fine roots extended out from the stream banks into the channel and were resistant to erosion (*Figure 12B*). Sediment sampling in zones with heavy root density could not cut through the plant matter and had to sample mid-channel sediments. As previously mentioned, knickpoints were often co-located with dense in-channel vegetation; as stream power and erosion concentrate over the knickpoints, the vegetation may eventually be eroded through.

We did not directly see many animals besides birds, but did see plentiful indirect evidence of beavers. Near Zones E5 and C5, deer fencing wrapped around trees indicated beavers are a concern (Location A on *Figure 7*). Upstream of the picnic area footbridge (Location C on *Figure 7*), a small woody debris jam and beaver-cut trees evidence recent beaver activity (*Figure 13A*). In the reach upstream, one team member (Swope) recorded a small fish (~1.5 inches long) swimming in Mesa Creek (*Figure 13B*). Although these observations are limited, we note that our team consists of geologists with no training in bird, plant, or other flora/fauna identification.

3.2.3 Summary

Historical photos attest to Mesa Creek being a dynamic braided channel that became single-thread as vegetation density increased. Although vegetation densification occurred across the watershed, it was most consistent in Zone 2, likely due to a steady base flow induced by Kissing Camels irrigation. Modern observations of vegetation indicate portions of the channel near Zone 3 have historically aggraded and killed large vegetation; downstream of this zone, current channel flooding is burying tree trunks but not causing die-off. Dense root mats stabilize channel banks. Aquatic and semi-aquatic habitat is sufficient to support beaver and small fish.

3.3 Sediment size

A central goal in this study is to analyze the grain size of the modern channel and the historical channel. Sediment size reflects: flow regimes, erosion rates and sources, and channel geometry. Prior work noted that sediment size decreases with urbanization (Russell et al., 2018), and the urban stream syndrome detailed in Chin (2006) focuses on sediment aggradation as a main symptom of urbanization. In order to

examine the effects of urbanization on Mesa Creek--including changing flow regimes due to urbanization and irrigation, erosion from construction, and resulting channel geometry alteration--sediment samples from the active channel bedload, floodplains, and terraces were analyzed for grain size distributions. Terrace and floodplain sediment provide important historical (pre-1937) baselines against which the modern Mesa Creek grain size distributions can be compared.

3.3.1 Methods

Sediment samples were collected from channel, floodplain, and terrace sites along Mesa Creek in Sondermann Park (*Figure 14, Table 2*). Each Rosgen classification reach (*Figure 7*) was sampled in the main channel. We chose the midpoint of each Rosgen reach, though this varied based on channel access, and co-located sediment samples with the channel cross sections used to calculate channel complexity (Section 3.4). Channel sections with armored beds or large pebbles to cobbles were avoided because those clasts were likely transported in large storm events rather than the normal flow regime. Highly vegetated sections proved difficult to sample due to thick root mats preventing bedload acquisition. The top inch (2-3 cm) of the bedload was collected from both the center and sides of the channel. Some clay, silt, and fine sand loss was unavoidable because these small grains would flow out of the collection trowel. However, clay and silt are removed from the historical and modern grain size comparison, following the methods in Stinchcomb et al. (2012), so this sediment loss has a minimal effect on results.

Table 2. Sediment sample sites

Sample ID	Latitude	Longitude	Location	Vegetation control	Channel type	D_{16}*	D_{50}*	D_{84}*
3-1-1	38.86422271	-104.8420435	Channel	Minimal	C4	0.44	1.67	4.18
3-1-2	38.86421559	-104.8419819	Floodplain	*n/a*	C4	0.29	0.7	2.71
3-1-3	38.86389084	-104.8418538	Channel	High	C6c-	0.42	2.75	9.42
3-1-4	38.8638464	-104.8418831	Floodplain	*n/a*	C6c-	1.09	2.21	4.47
3-1-5	38.86253388	-104.8410656	Channel	High	DA6	0.23	1.41	4.07
3-1-6	38.86253388	-104.8410656	Floodplain	*n/a*	DA6	0.37	1.63	4.06
3-1-7	38.8618075	-104.8405254	Channel	Minimal	DA6	0.31	1.54	6.61
3-2-9	38.86216377	-104.8407664	Channel	High	C6c-	0.26	1.32	2.32
3-2-10	38.8617307	-104.840226	Channel	High	DA6	0.22	2.01	4.62
3-2-13	38.85910641	-104.8388258	Channel	Minimal	DA5	0.24	1.45	3.6
3-2-14	38.85910641	-104.8388258	Terrace	*n/a*	DA5	0.13	0.68	2.11
3-2-15	38.85880854	-104.8384691	Terrace	*n/a*	B5c	0.08	0.43	2.18
3-2-16	38.85880854	-104.8384691	Channel	Minimal	B5c	0.07	0.25	1.14
3-2-17	38.85836325	-104.8386359	Terrace	*n/a*	E5	0.09	0.38	6.56
3-2-18	38.85830385	-104.8384357	Channel	High	E5	0.37	2.01	7.1
3-2-19	38.85751757	-104.8382439	Terrace	*n/a*	C4	0.22	1.02	5.07
3-2-20	38.85762645	-104.8382841	Channel	Minimal	C4	0.44	2.49	6.82

* calculated without fines for floodplain and terrace samples

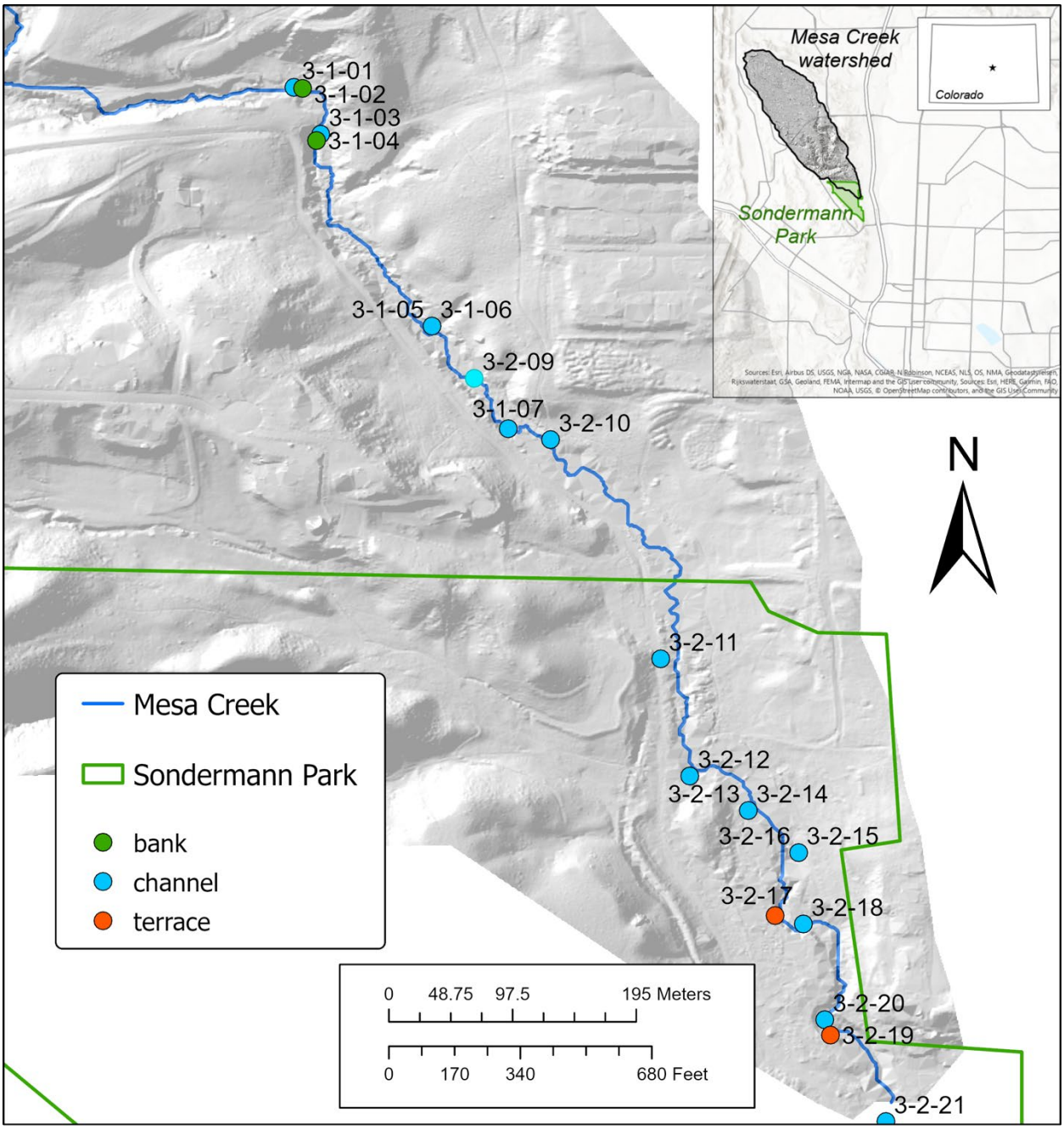

Figure 14. Location of sediment sampling sites along Mesa Creek. Bank and floodplain samples are synonymous. Overlapping symbology includes: Sample 3-1-6 that is a bank sample, and Samples 3-2-14 and 3-2-15 that are terrace samples.

Figure 15. Example of good and bad terrace sampling. Pictured location is sample 3-2-19.

Historic sediment samples were taken from terraces and floodplains. Distinct terraces are only found within the Sondermann Park boundaries, so three floodplains were sampled in the upstream reach of our focused study area (*Figure 14*). Terrace samples were taken by digging directly into the side of the terrace, which was exposed in cut banks. We preferentially sampled under roots and in exposed surfaces to minimize contamination by uphill colluvium (*Figure 15*). Samples were taken approximately 5 inches into the cut bank to further avoid contamination.

In reaches of the modern channel where there weren't clear terraces, floodplains were sampled instead. Samples were collected from at least 8.7 inches (22 cm) below the surface to avoid overbank deposition and capture historic bedload. Although we intended to collect a historical sample at every modern sample site, frozen ground and thick root mats prohibited collection except at the upstream and downstream ends of our study area (*Figure 14*).

All samples were collected using hand trowels, then placed into labeled ziploc bags to be dried and sieved in the labs at Colorado College. Each sediment sample was labeled month - day - number (mm-dd-##). Enough material was collected so that the mass of the largest clast was less than one percent of the total weight of the samples; each sample weighed at least ~500g when dried (Bunte and Abt, 2001).

Twenty samples in total were collected and dried in phases. First, the sediment was dried in large baking-pans in the sun, so that excess stream water would evaporate. Then, samples were transferred to smaller containers and cooked in a drying oven until no moisture was left. This process took ~12 to 48 hours for channel sediments, while terrace and bank samples required 6 to 12 hours to completely dry out. The dry weight of each sample was taken before sieving.

Each sample was sieved through a standard set of sieves, except 0.71 mm and 0.125 mm meshes, using a Rototap machine to disaggregate and sort the grains. Each sample was mechanically sieved for 10 minutes, then the grains captured in each sieve were weighed and recorded to capture the grain distribution. All grains larger than the 4 mm sieve had to be hand sorted due to missing sieves of >4 mm mesh. Mud-heavy samples (3-2-09, 3-2-10, 3-2-15, 3-2-16) were not completely broken up by the Rototap and contained large cohesive mud clasts. A mortar and pestle were used to break up the mud clasts, then those samples were sieved, sorted, and weighed again.

After drying, sieving, and weighing was complete, sediment size distributions were created using the percent weight; these were compiled into Probability Distribution Function (PDF) and Cumulative Distribution Function (CDF) plots for each site.

3.3.2. Results

3.3.2.1. Modern Channel

We collected and analyzed sediment samples for ten in-stream sites (*Figure 16*). Median grain size or D50 ranges from 0.25 to 2.75 mm, indicating that the median size in Mesa Creek ranges from medium sand to very fine gravels. In contrast to abrasion theory, grain size in Mesa Creek does not decrease with distance downstream nor display any systematic trend in space. Likely, this reflects: 1) short travel distances which do not impact abrasion potential; 2) tributary inputs of coarser sand, particularly in tributaries draining the Mesa Gravel capped hills and trails; or 3) variability in sediment transport potential along the stream. Interestingly, the lowest D50, which is significantly smaller than the 1.4-2.75 mm range of the other nine samples, is found in the B5c Rosgen reach. This reach is noted for being moderately entrenched as compared to the minor entrenchment of the other reaches, contains 2x steeper slope than other reaches, and is just downstream of a large knickpoint.

The range in size between D16 and D84 reflects how well or poorly sorted the stream sediments are. Similar to the D50, there is no systematic change in grain size range from upstream to downstream in our study area (*Figure 17*). Grain size range is between 1.06 mm up to 9 mm. The highest range is associated with the highest median grain size, while the lowest range is associated with the lowest median grain size. Most reaches show a range between 2-7 mm, which reflects medium sands to fine gravels in the active channel. The smallest range, in Rosgen reach B5c, is in a moderately entrenched zone with a low D50. This is the only moderately entrenched zone in the study area, and the low grain size and range particular to this reach suggests that greater entrenchment in Mesa Creek leads to lower grain sizes. Unintuitively, the lidar slope analysis revealed reach B5c to have twice as high a slope as the rest of the study area; theoretically this should lead to higher transport capacity and larger grain sizes. That it doesn't may indicate errors in the lidar, which is interpolated in regions of high canopy cover, or a disconnect between the channel bed and transport potential.

The relationship between Rosgen reach and grain size is further explored using the CDFs for the ten channel sites (*Figure 18*). Rosgen type DA corresponds to multi-threaded channels shown in *Figure 18A*, while single thread channels are grouped in *Figure 18B*. The multi-threaded channels tend to have more similar grain size distributions, as reflected by the tighter range in D16, D50, and D84 values. These range from 0.21 to 0.44 mm, 1 to 2.49 mm, and 3.6 to 6.82 mm, respectively (*Figure 18A*). In contrast, single-channel

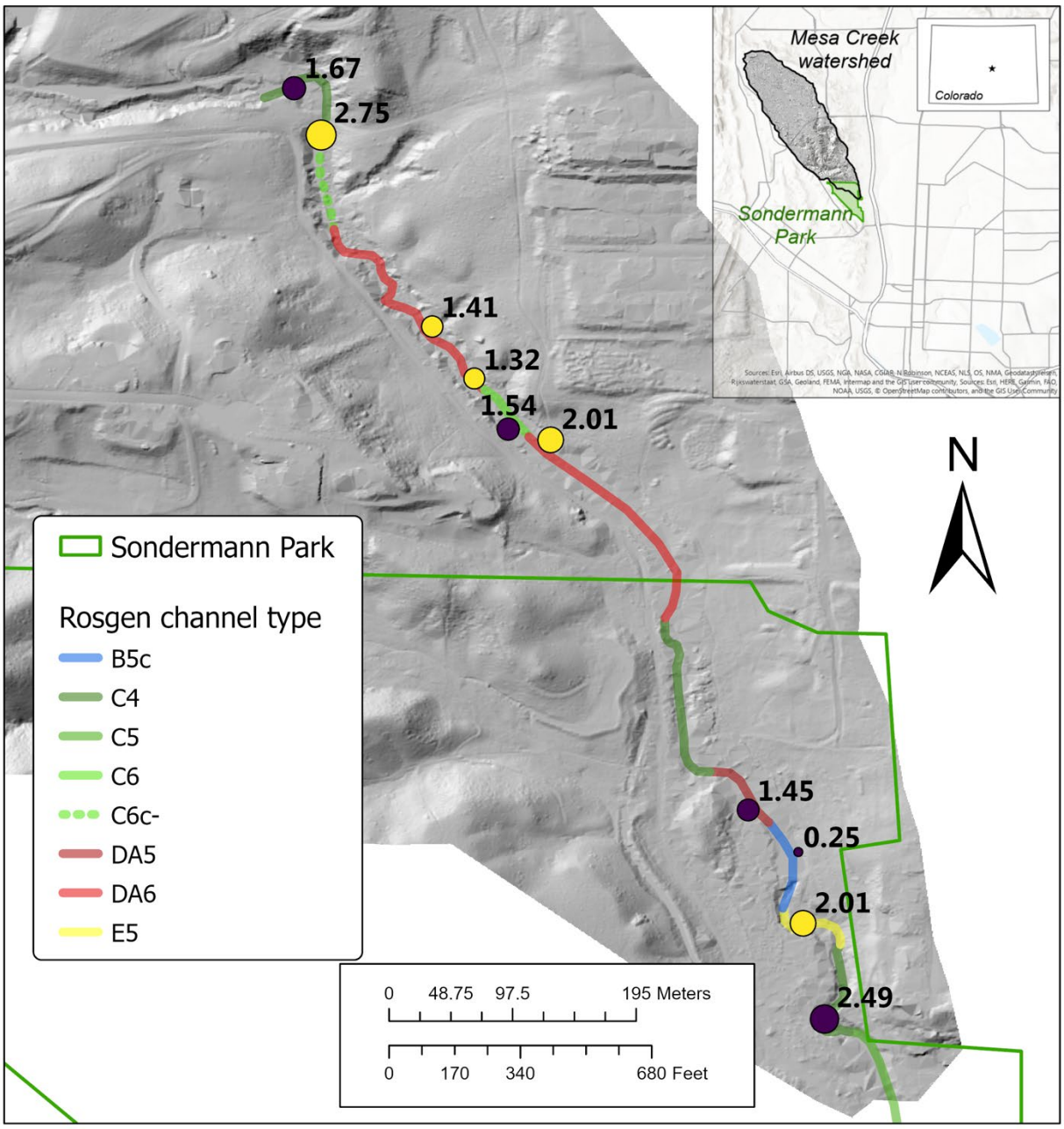

Figure 16. Median sediment size (D_{50}) for channel samples in mm. Size of symbol is proportional to grain size in mm. Yellow indicates a strong vegetation control on channel form, while dark blue is a weak vegetation control. Rosgen channel classifications shown for reference.

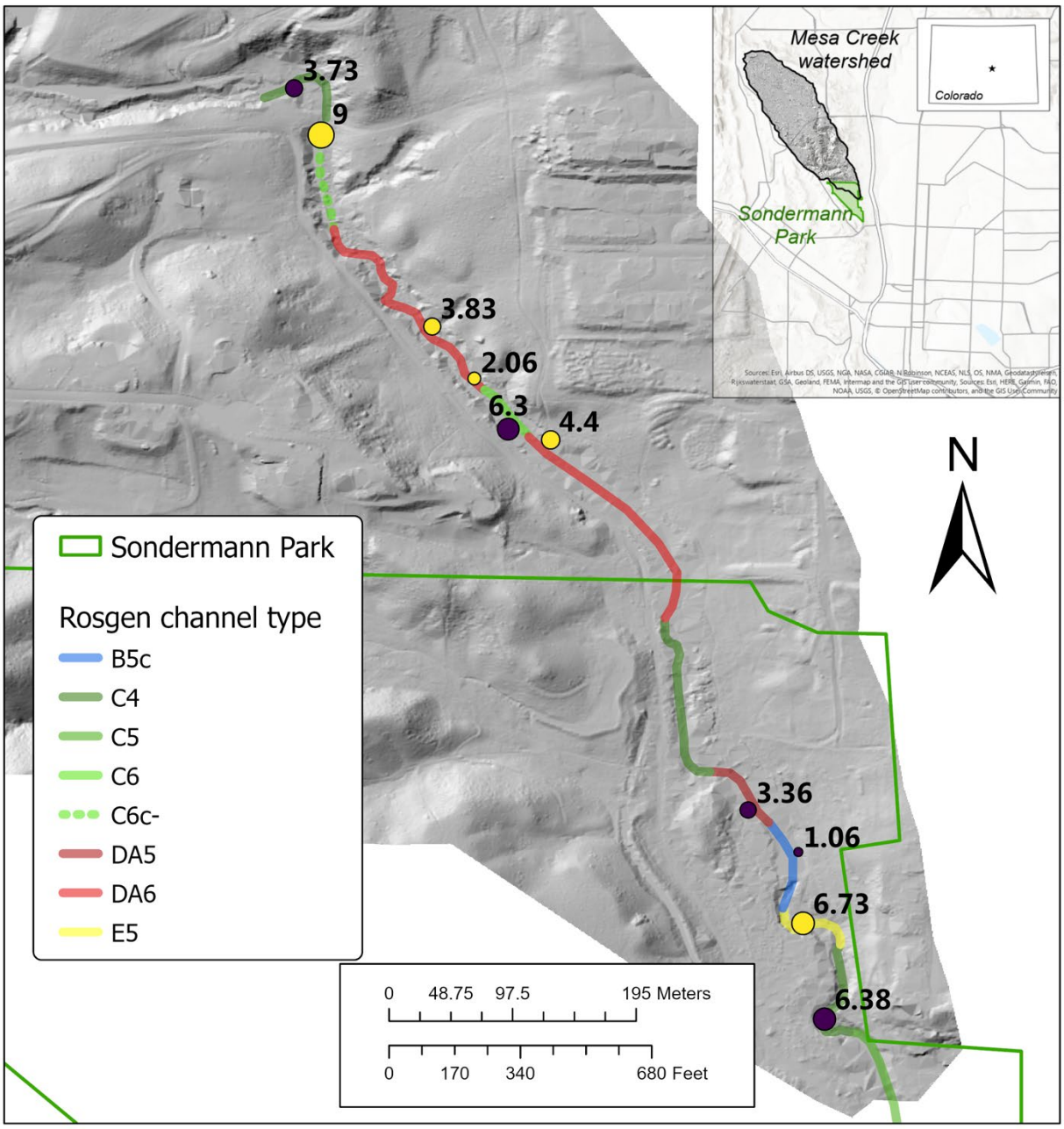

Figure 17. Difference between D_{84} and D_{16} (standard deviations from mean) for each channel sample shown, in mm. Yellow represents channel reaches with strong vegetation control on form, while dark blue indicates a weak vegetation control. Rosgen reach classifications shown for reference.

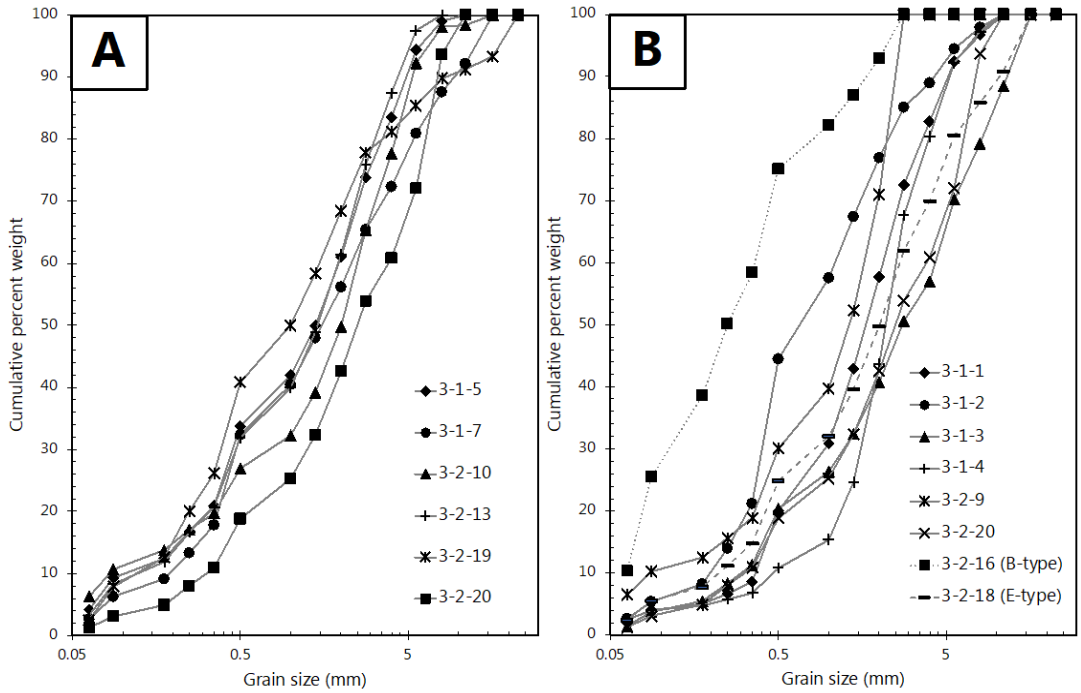

Figure 18. Cumulative distribution functions split for A) multi-thread channel types, equivalent to Rosgen type DA, and B) single-channel types. Grey bars show the range of values for D_{16}, D_{50}, and D_{84}. Panel B bars exclude the B and E channel types and only use C channels.

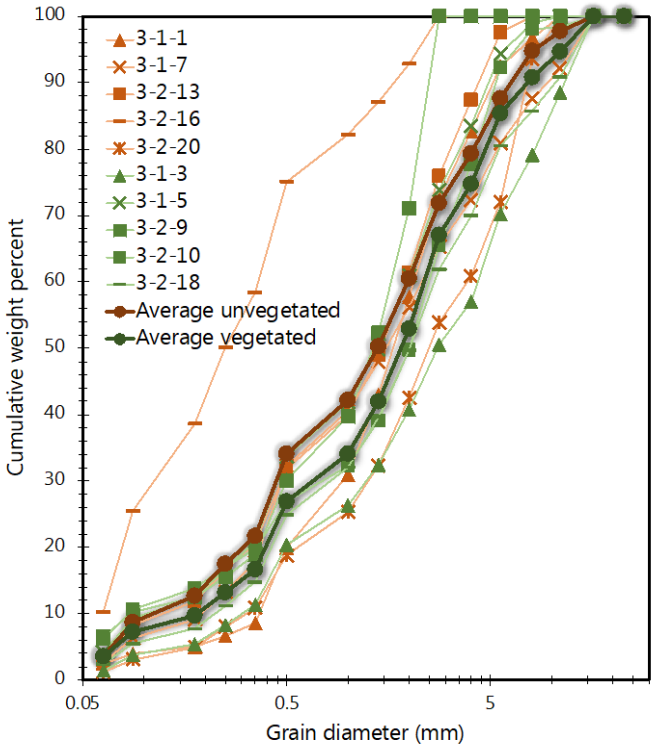

Figure 19. Channel grain size distributions grouped by vegetation control.

reaches display wider variability in grain sizes. Most single-thread reaches are type C, with two exceptions: a B channel reach that shows overall much lower grain sizes and is distinguished by greater channel entrenchment, and an E channel reach—noted for higher sinuosity—with similar grain size distributions as the C reaches. Considering only the C channel types, the range in D16, D50, and D84 is nearly twice that of the multi-thread channels: 0.26 to 1.02 mm, 0.67 to 2.75 mm, and 2.32 to 9.42 mm. These results indicate that while grain size and multi-threaded channel types may be linked, single-thread channels in Mesa Creek can display a wider range of grain sizes.

Finally, channel samples are grouped by degree of vegetated control (*Figure 19*). Vegetation control is spread throughout the study area, with no spatial clustering of regions with high vegetation control (*Figure 16, Figure 17*) and is not associated with particular Rosgen classifications. Unlike the Rosgen grouping, the grain size distributions for channels with and without vegetative control are relatively similar (*Figure 19*). Average distributions have a similar shape, though the unvegetated distribution is systematically a few mm smaller than the vegetated channel type. Within error, however, there is no apparent difference in the grain size distributions between channels with and without vegetation. However, it's important to note that our results here may be biased by the fact that sediment collection was inhibited in channels with thick vegetation mats and so our results only show channels with no to moderate vegetative influence.

3.3.2.2 Historic channel

Seven sediment samples were collected from floodplains and terraces: three from floodplain deposits in the upstream half of the study area, and four from terrace deposits in the downstream half of the study area. In the following sections, we remove fine sediment <0.0625 mm as this can reflect soil development rather than sediment transport processes (Stinchcomb et al., 2012). The fine fraction is also removed from any channel sites that we compare with historical sediment data.

Floodplain samples tend to have a higher median grain size than terraces, though this trend is not systematic (*Figure 20*). Median floodplain grain sizes range from 0.7 to 2.21 mm, and represent coarse sands to very fine gravels. Terrace sediment D50 ranges from 0.38 to 1.02 mm and corresponds to medium to coarse sands. It's unclear if the size difference reflects changes in sediment transport between floodplain and terrace formation, presuming that terrace sediment reflects older sediment transport conditions than floodplain sediments do, because the two deposit types are found in spatially distinct regions. Therefore, the smaller median grain sizes of the terraces could reflect downstream fining, increased fine contributions from tributaries, or lower transport capacity due to a lower slope.

While the median grain size of terrace deposits are finer, they also display a wider range of sizes (*Figure 21*). Floodplain deposits range from 2.42 to 3.69 mm, while terrace deposits range from 1.98 to 6.48 mm. This suggests terrace deposits are poorly sorted and may represent a much wider range of sediment transport conditions than the floodplain deposits.

To delve into the changing hydrology and geomorphology of the modern Mesa Creek, we compared floodplain and terrace deposits to the paired channel deposits. The paired samples were taken within a range of 10 feet from each other, and allow us to directly compare how the grain sizes differ between modern and

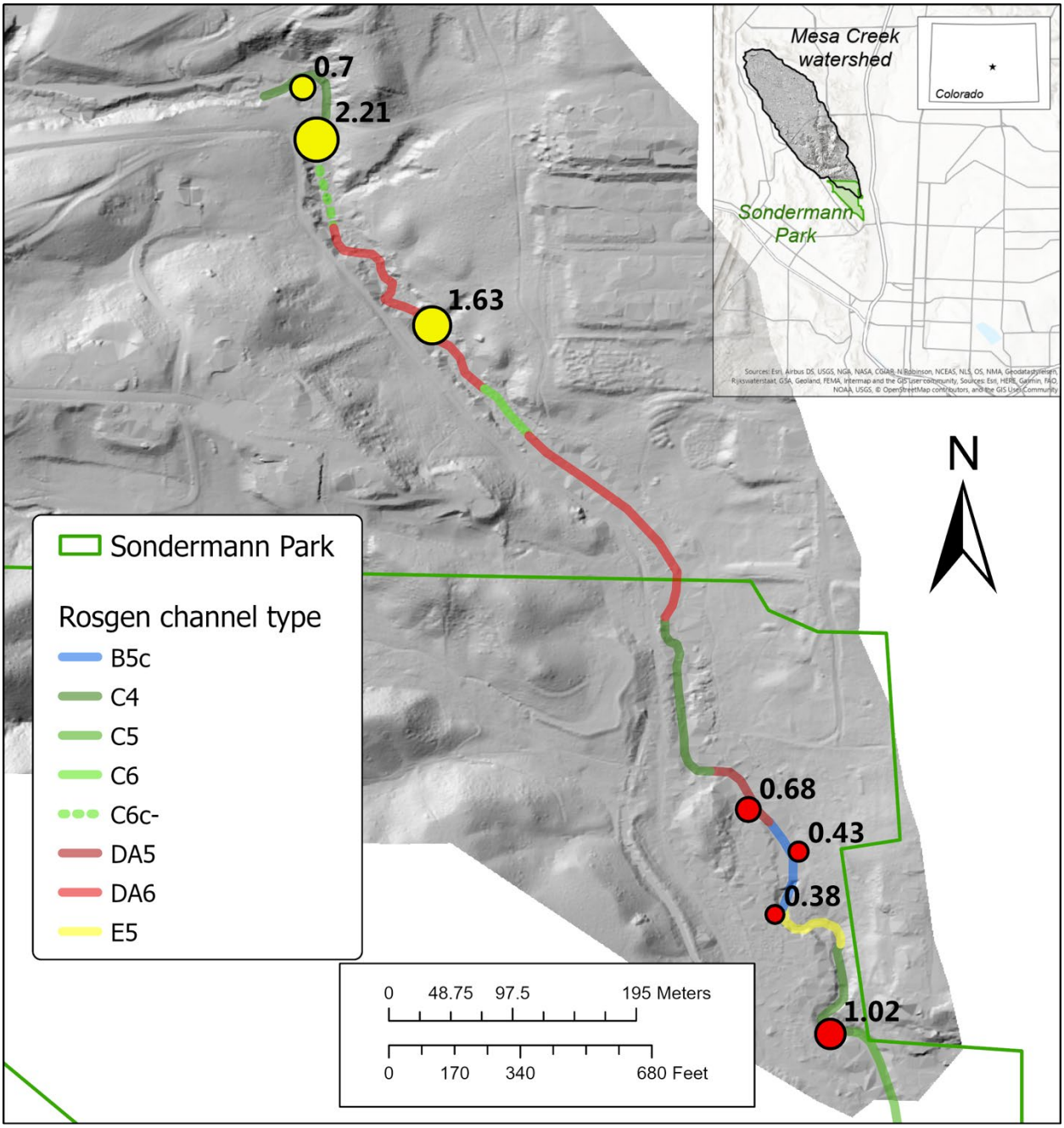

Figure 20. Median grain size (D50) for floodplain and terrace samples in Mesa Creek. Yellow are floodplain samples while red are terrace samples. Size of symbol corresponds to the grain size, as labelled in mm.

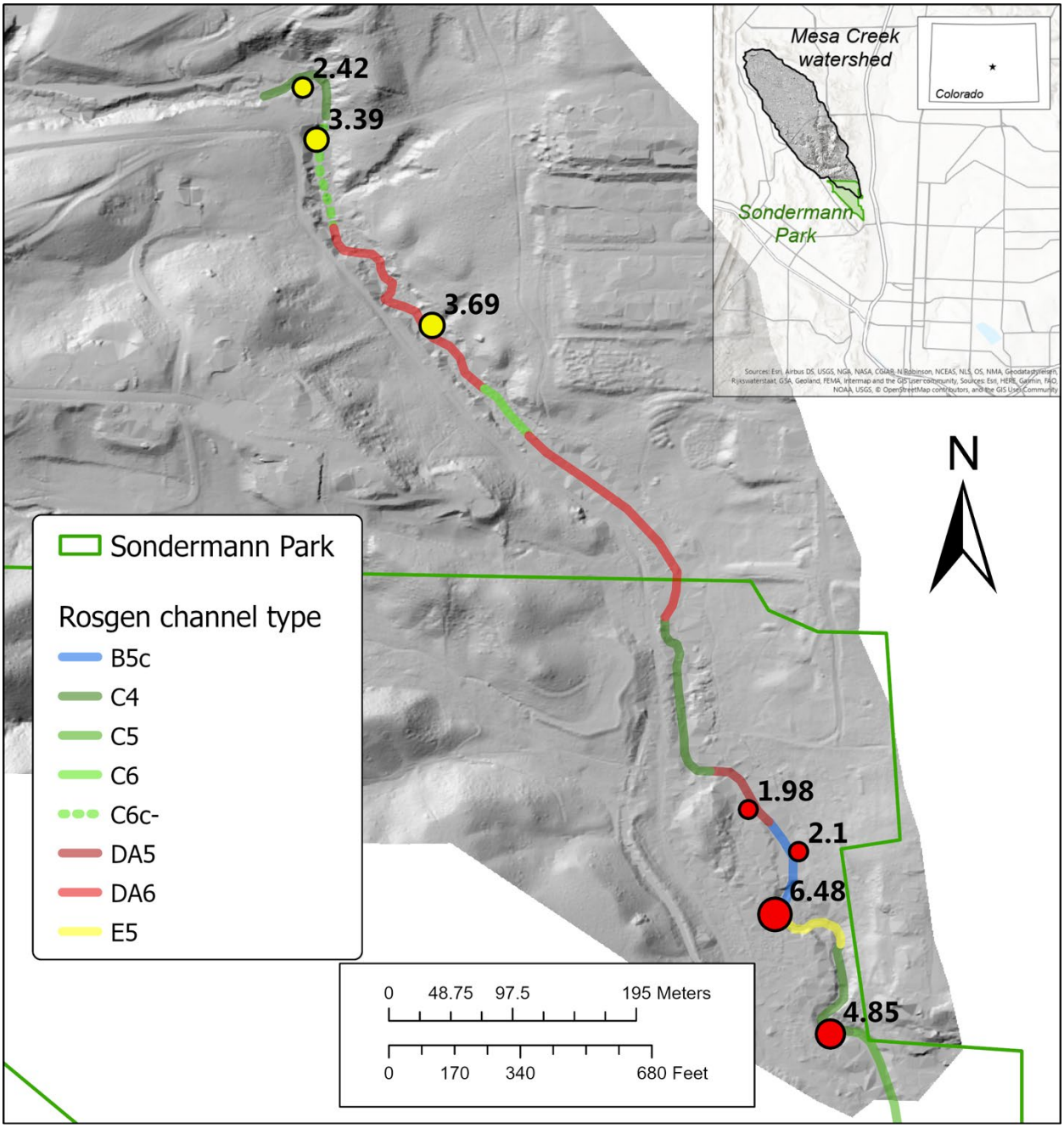

Figure 21. Range in grain size from D84 to D16 for floodplain (yellow) and terrace (red) sediment samples. Size of symbol corresponds to range, also labelled in mm.

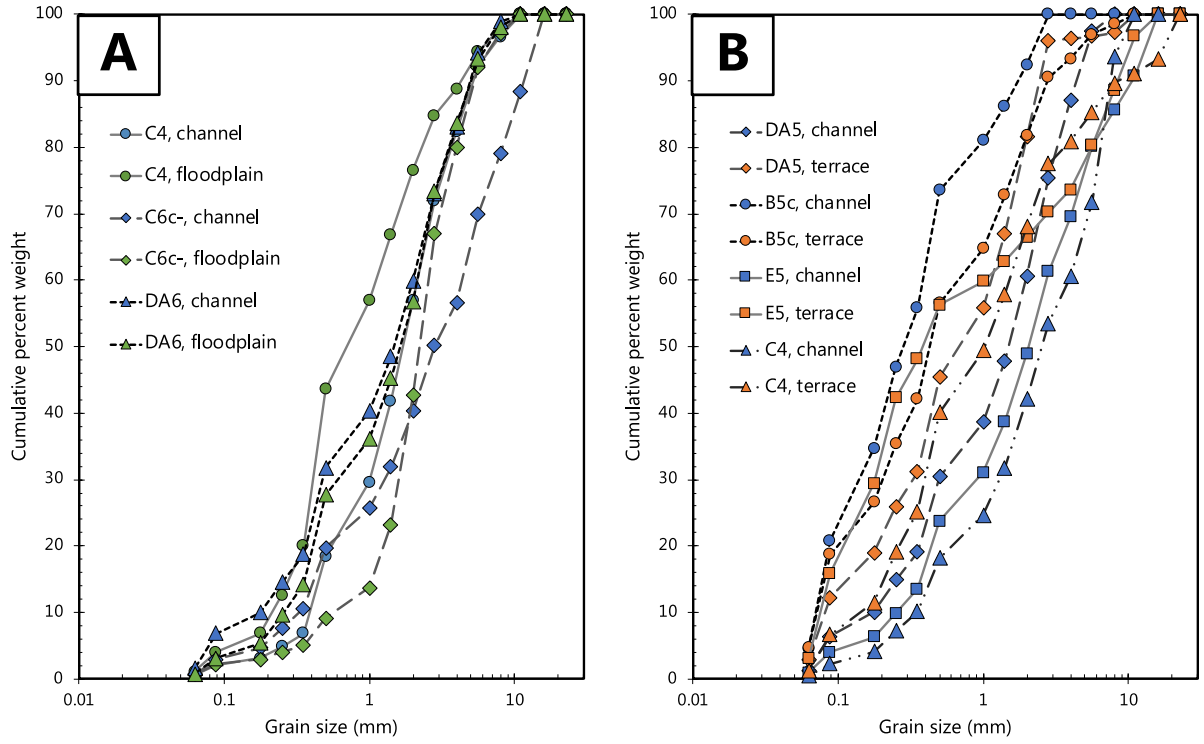

Figure 22. Grain size distribution comparisons for A) channel and floodplain samples and B) channel and terrace samples. Channel samples are noted in blue, floodplain in green, and terrace in orange. Symbols in each panel are similar between paired sample sites.

historic deposits. This in turn will allow us insight to how the hydrology and geomorphology of Mesa Creek has changed.

Floodplain deposits are generally finer grained than the modern channel (*Figure 22, Table 3*), though the multithreaded DA6 samples show an opposing trend. At the upstream C4 reach, the channel deposits are over a mm larger for most of the distribution; in contrast, the DA6 reach is within less than a mm difference, suggesting very little change in the grain size distribution over time. However, a two-sample Kolmorov-Smirnov test indicates that all floodplain samples are significantly different than the channel samples with $D_{n,m}$ of 27.32, 23.35, and 4.89 for the C4, C6c- and DA6 reaches, respectively and a $D_{n,m,a}$ of 0.06.

With the exception of reach B5c, the terrace analysis also shows coarser modern channel bedload relative to the historic terrace deposits. This can be seen strongly in *Figure 22*, as all the orange terrace distributions are shifted left relative to the channel sites. Two sample Kolmorov-Smirnov tests again indicate that terrace sample distributions are significantly different than the channel samples with $D_{n,m}$ of 20.94, 16.99, 34.62, and 26.14 for the DA5, B5c, E5, and C4 reaches, respectively and a $D_{n,m,a}$ of 0.06. The one instance where terrace deposits are coarser than modern channel is in reach B5c, which is the moderately entrenched zone just below a knickpoint. This reach also had the lowest modern grain size distribution and so the relatively coarser terrace deposits may just reflect the anomalously smaller modern grain sizes.

The contrast in historic and modern channel deposits is further elucidated when the frequency of each grain size bin is compared for modern, floodplain, and terrace samples (*Figure 23*). Floodplain and channel

Table 3. Difference in grain size (channel minus floodplain/terrace) in mm.

	C4 3-1-1 & -2 Floodplain	C6c- 3-1-3 & -4 Floodplain	DA6 3-1-5 & -6 Floodplain	DA5 3-2-13 & -14 Terrace	B5c 3-2-15 & -16 Terrace	E5 3-2-17 & -18 Terrace	C4 3-2-19 & -20 Terrace
D16	0.17	**-0.65**	**-0.08**	0.14	0.00	0.29	0.24
D50	1.01	0.57	**-0.16**	0.82	**-0.15**	1.68	1.50
D84	1.51	4.99	0.06	1.52	**-0.94**	0.65	1.77

samples have similar frequencies across all grain sizes, with a bimodal distribution in each. Channel deposits tend to contain higher percentages of coarse grains in the gravel grain size, though the difference in channel and floodplain deposits is within error of both samples. In contrast, clear differences emerge between channel and terrace deposits. Terraces contain higher frequencies of fine to medium sands with almost twice the average frequency (5 versus 10%). In contrast, the channel has ~5% greater frequency of fine gravels in the 3-10 mm range. Both samples converge to have similar frequencies of medium gravels 10 mm or greater in diameter. Like the upstream paired floodplain and channel samples in *Figure 23A*, the downstream paired terraces and channel samples are bimodal, though the modality is not as clearly defined due to enrichment in fine (terrace) and coarse (channel) sediments.

We interpret these trends to indicate that the transport capacity between floodplain and channel has not changed significantly, as these deposits have similar trends in *Figure 23* and no consistent change in grain size in *Table 3* and *Figure 22*. However, the transport capacity has altered between the deposition of terrace sediments and the modern channel, as seen by the consistent coarsening of deposits with time in *Figure 22* and *Table 3*, and the clear shift in frequency of finer and coarser material in *Figure 23B*. That a higher proportion of finer material and a lower proportion of coarse material is present in terraces suggests that the transport capacity was lower historically and has since increased. Since transport capacity relies on

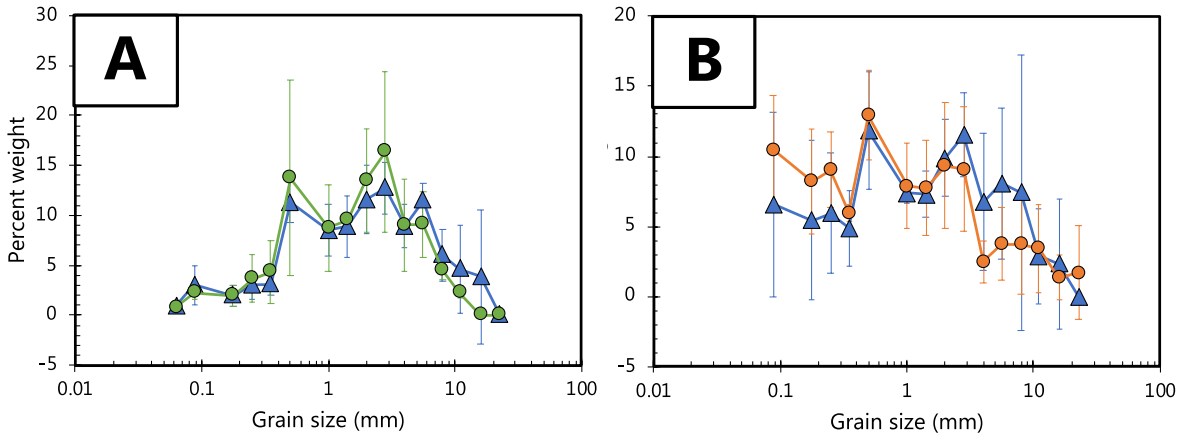

Figure 23. Grain size comparisons at each sieve size for A) paired channel and floodplain and B) paired channel and terrace deposits. Channels are noted with blue, while floodplains are green and terraces are orange.

basal shear stress, this indicates that over time, shear stress has increased through either 1) increased discharge, 2) decreased channel width, 3) increased channel slope, or a combination thereof (*Figure 24*).

The grain size distributions through time reflect a bimodal sediment size that peaks at a coarse sand and fine gravel. This bimodality likely reflects the surrounding geology. Erosion of Mesa Gravels contributes gravel to coarse sand-sized clasts of Pikes Peak Granite which is relatively resistant to erosion. In our hand-counts, nearly all of the >4 mm clasts were composed of granite or of the granite's mineral constituents. Below the Mesa Gravels lies the Pierre Shale, which erodes in floccules or clasts composed of clay and silt particles. These particles compose most of the fine to coarse sand deposits, as well as the fine deposits less than 0.0625 mm.

3.3.*3* Summary

The modern Mesa Creek channel contains clasts ranging from fine sand to pebbles, with median sizes frequently in the medium to coarse sand range. Multi-threaded channels classified as Rosgen reach type DA have similar grain size distributions across the Mesa Creek study area; in contrast, single thread channels of Rosgen type C tend to have twice as much variability in grain size distributions. This suggests that grain size and multi-threaded channels are related, though it is unclear whether the grain size distribution causes multi-threaded channels or vice-versa.

Of the single-threaded channels, the Rosgen reach B5c was an outlier with a much smaller median grain size, a tighter grain size distribution, and a decrease in grain size from historic to present. This reach is moderately entrenched compared to the low entrenchment of the rest of the study area and is created by the passage of a knickpoint located at the upstream end of the reach. That grain size differs so strongly here is likely due to a decrease in transport capacity caused by knickpoint passage, and points to the need to mitigate knickpoint migration in order to maintain the medium to coarse sand distribution.

In comparing floodplain and terrace deposits to the modern channel, we find little difference between floodplain and the modern channel. However, terrace deposits contain more fines and fewer coarse material, indicate a lower transport capacity historically. This could be due to lower discharge, wider channels, or lower slopes in historic times. Comparison of historic and modern deposits also shows a consistent bimodality in grain size distributions that reflects the geology of the region: Mesa Gravels and Pikes Peak Granite tend to form fine gravels while the Pierre Shale forms medium to coarse sands composed of clay and silt floccules.

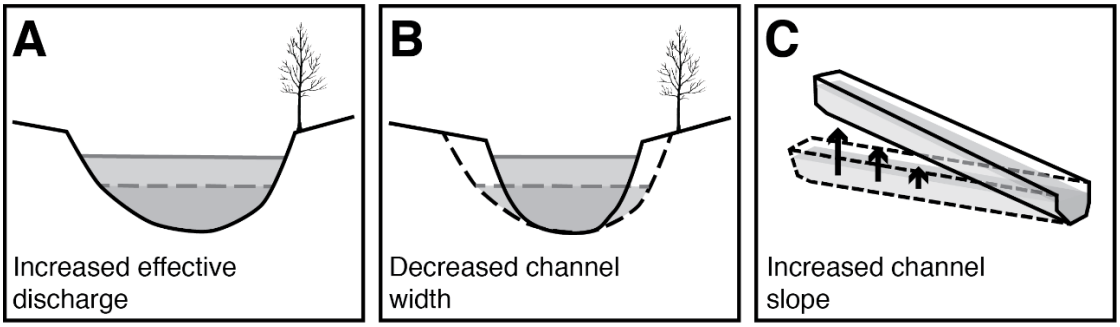

Figure 24. Three possible scenarios to explain the increase in transport capacity from terrace deposits to modern channel deposits. Dashed lines indicate historic conditions during terrace formation.

3.4 Channel Complexity

Channel complexity is the quantification of the variability of an aspect of a stream, such as width, depth, or bedload. These metrics can be examined at the scale of a reach, or across the entire length of the stream. Urban streams tend to have reduced complexity compared to their unaltered counterparts. This is considered to be due to "urban stream syndrome"; rectangular channels, poor bed load complexity, and homogeneous vegetation are common for streams with urbanized watersheds (Booth et al., 2016). Complexity is important for aquatic habitat; more complex channels can support more wildlife and greater biodiversity due to a greater range of environments within the channel (Laub et al., 2012). Here, we build on sediment size measurements and add new channel geometry measurements to quantify the channel complexity at Mesa Creek.

3.4.1 Methods

Channel cross-sections were measured using standard surveying techniques with a stadia rod, hand level, and tape measure. Channel cross-section sites were selected after every change in Rosgen classification within the study area (*Figure 25*). Within a Rosgen classification zone, survey sites were selected to be representative of the channel morphology within the zone. In order to compare bedload with other complexity metrics, many of the cross-section sites coincide with sediment sampling sites (*Figure 14*).

The longitudinal profile of Mesa Creek was extracted using ArcGIS and the 2 ft lidar DEM. A longitudinal profile compares the elevation of the stream at regular points along the center of the channel to the distance upstream. The 2 ft lidar DEM was processed using ArcGIS Pro hydrology tools to find the channel centerline as a vector, with which the DEM elevations were extracted. The distances and elevations were exported to Excel for plotting and analysis.

Channel complexity in Mesa Creek was quantified with one metric specific to each of width, depth, and bedload, along with qualitative analysis of the longitudinal profile. The metric chosen for channel width complexity was the coefficient of variation of width (CVW) (Laub et al., 2012). Channel width is defined as the distance between the top of the geomorphic banks, perpendicular to the direction of flow. CVW is the standard deviation of width divided by mean width, and acts as a metric of the variability of channel width. CVW was calculated for the entire study area, and cumulatively from the upstream to downstream reaches. Similarly, the metric chosen for channel depth was the coefficient of variation of depth (CVD), which is standard deviation of depth divided by mean depth. Channel depth is the vertical distance between the top of the geomorphic banks to the point within the wetted channel. CVD was calculated for each channel cross-section. CVD can be used as a proxy for channel rectangularity, as an entirely rectangular wetted channel would have a CVD of 0. The metric chosen for bed load complexity was the gradation coefficient, which is calculated using D_{16}, D_{50}, and D_{84}:

$$s_{grad} = \frac{\frac{d_{84}}{d_{50}} + \frac{d_{50}}{d_{16}}}{2}$$

Gradation coefficient is a measure of the spread of bed sediment distribution. Lower gradation coefficients represent narrower grain size distributions. For statistical analysis, t-tests were used when comparing categorical variables to numerical variables, and linear regression models were used when comparing two numerical variables. All statistical significance values are expressed as p-values.

3.4.2 Results

3.4.2.1. Channel width

Channel width generally increases from upstream to downstream with minimum widths of one meter to maximum widths of 3 meters (*Table 4*). The cumulative CVW also increases overall, as would be expected in most cumulative CVW plots; as more datapoints are integrated downstream, the variance is expected to increase. Width should also increase downstream following global empirical channel width – drainage area scaling laws, which would further increase the CVW in the downstream direction. This expected trend is observed between sites 1 and 6. However, the CVW rapidly increases between channel ID 6 and 7, corresponding to the upstream wooden bridge and picnic area within Sondermann Park (*Figure 25*). This area is currently ponded, as seen in the multiple wide channels in Channel ID 7. The cumulative CVW remains high for the rest of the study area, but does not increase with distance; this is a result of the large disturbance in CVW presented by channel ID 7, as channel widths in ID 8-11 do show variation (*Table 4*).

Table 4. Channel complexity metrics for Mesa Creek

Channel ID	Rosgen classification	Vegetation control	Channel width (m)	Cumulative coefficient of variation of width	Coefficient of variability of depth	Bedload gradation coefficient
1	C4	weak	1.22	--	0.06	3.9
2	C6c-	strong	1.35	0.07	0.39	5.08
3 - west	DA6	strong	0.98	0.16	0.39	4.76
3 - east		strong	1.1		0.2	
4	C6	strong	1.15	0.13	0.21	3.35
5 - west	DA6	strong	1.34	0.18	0.19	6.18
5 - center		strong	0.85		0.34	
5 - east		strong	0.85		0.32	
6	C4	weak	1.37	0.18	0.14	--
7 - west	DA5	weak	3	0.45	0.11	4.58
7 - center		strong	1.05		0.89	
7 - east		strong	2.05		0.57	
8	B5c	weak	2.97	0.49	0.04	3.99
9	E5	strong	2.36	0.48	0.29	4.63
10	C4	weak	1.43	0.47	0.03	4.1
11	C5	weak	2	0.45	0.04	--

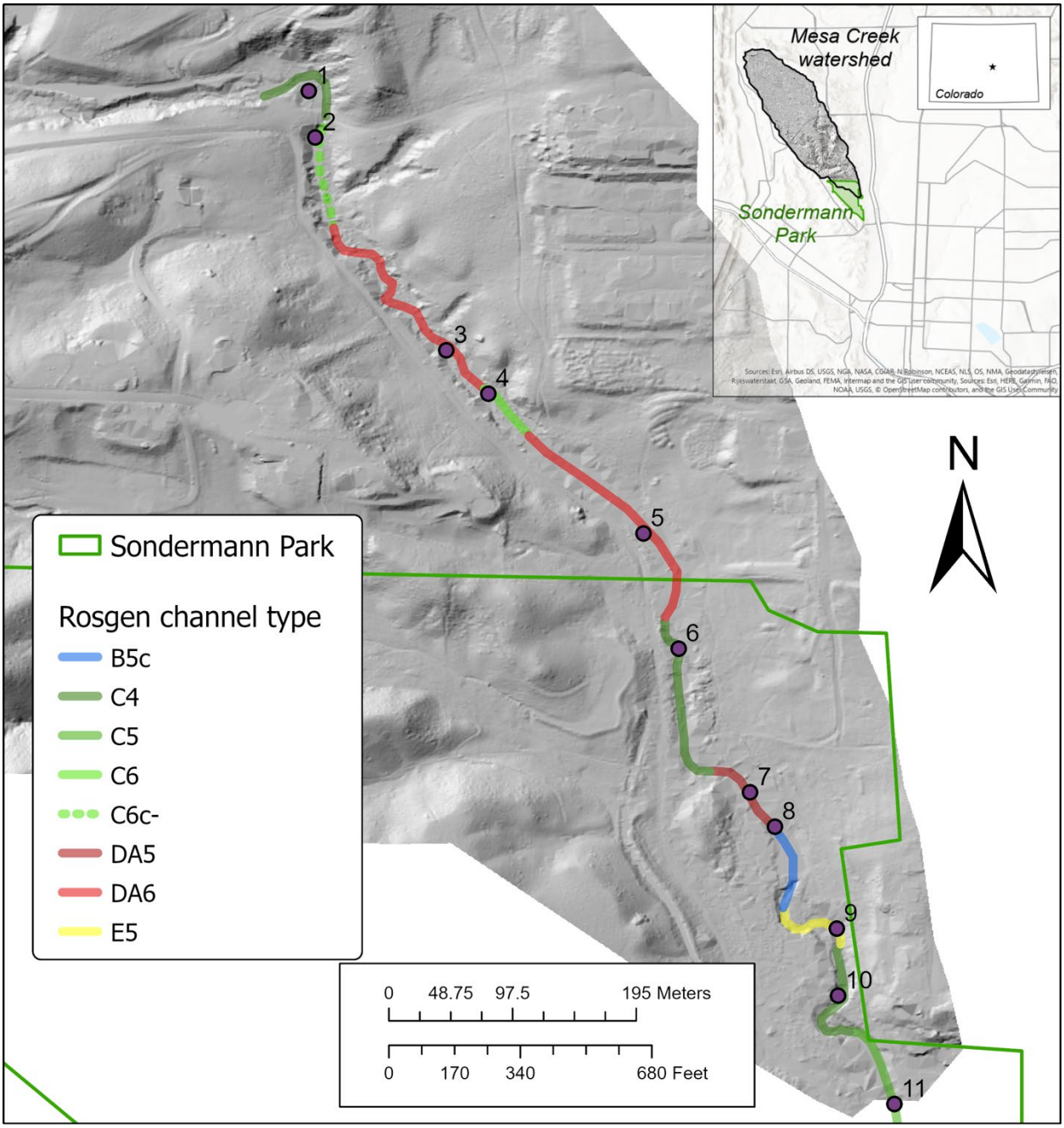

Figure 25. Location of channel cross section surveys for channel complexity metrics. At sites 1 and 10, the surveys included floodplains; sites 2-9 only surveyed the active channel from bank to bank.

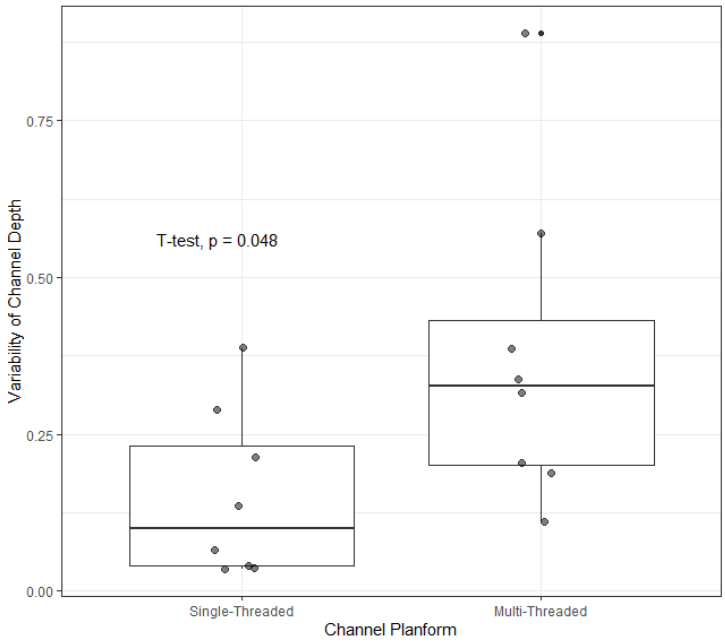

Figure 26. CVD compared to channel type. Single threaded channels correspond to Rosgen types B, C, and E, while multi-threaded channels correspond to Rosgen type DA.

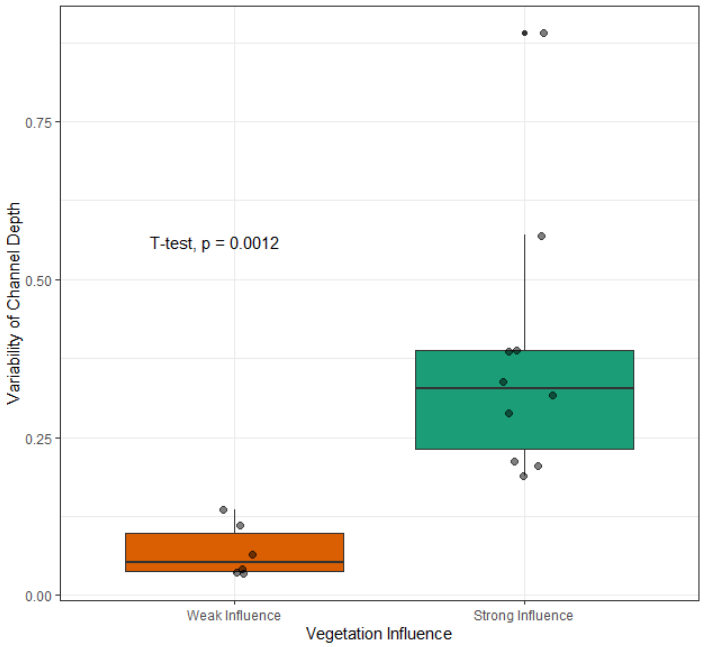

Figure 27. Boxplot of CVD compared against vegetation influence on the channel.

3.4.2.2. Channel depth

There are no clear trends in the coefficient of variability of depth (CVD) from upstream to downstream (*Table 4*). The lowest CVD values are found at the reaches near the upper and lower ends of the study area, suggesting these regions tend to have more rectangular and less complex channels. The multi-threaded channels tend to have greater CVD values and also a broader range of CVD values (*Figure 26*). This difference in means is statistically significant, with a p-value of 0.048. Thus, while there are no trends in

the spatial variability of CVD, there is a difference in CVD between single and multi-threaded channels. Multi-threaded channels in Mesa Creek are likely to have a broader range of channel depths, and thus greater channel complexity, within a cross-section.

We can additionally compare the influence of vegetation on depth complexity. Here, the contrast is even stronger, with a highly significant difference in CVD between channels with a weak and strong vegetation influence (*Figure 27*). The unvegetated reaches all have CVDs of less than 0.14, which indicates that they all have highly rectangular channel cross-sections. Conversely, vegetated channels have higher variability than unvegetated channels and are a significantly different population with a p-value of 0.0012. The variability in vegetated channels also has a wider distribution, as indicated by the wider spread of the box and whiskers plot. This indicates that the lack of vegetation creates uniform channel cross-sections, and that channel vegetation can add geomorphic complexity. That vegetation differences exert a more significant control than channel type suggests that the vegetation is a more direct control on depth complexity than channel type.

3.4.2.3. Channel bedload

Similarly, there is a difference between gradation coefficient in vegetated and unvegetated channels (*Figure 28*). Gradation coefficients for unvegetated and weakly vegetated channels is approximately 4, with little variance. In contrast, the vegetated channels have gradation coefficients ranging from 3.25 to 6.25, with a median of 4.7. The p-value of this difference is 0.096, so the difference is moderately, but not strongly, significant. This is in contrast to the strong significance between channel depth complexity and vegetation, but is also consistent with our earlier grain size analyses that found qualitatively only moderate differences in the CDFs of vegetated and unvegetated channels (*Figure 19*).

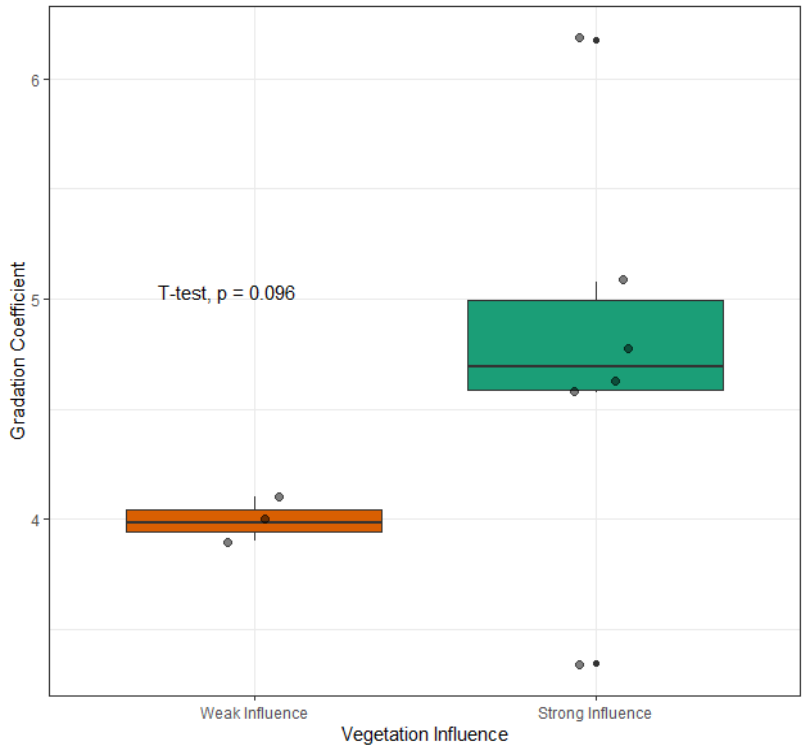

Figure 28. Boxplot of the bedload gradation coefficient against the vegetation influence.

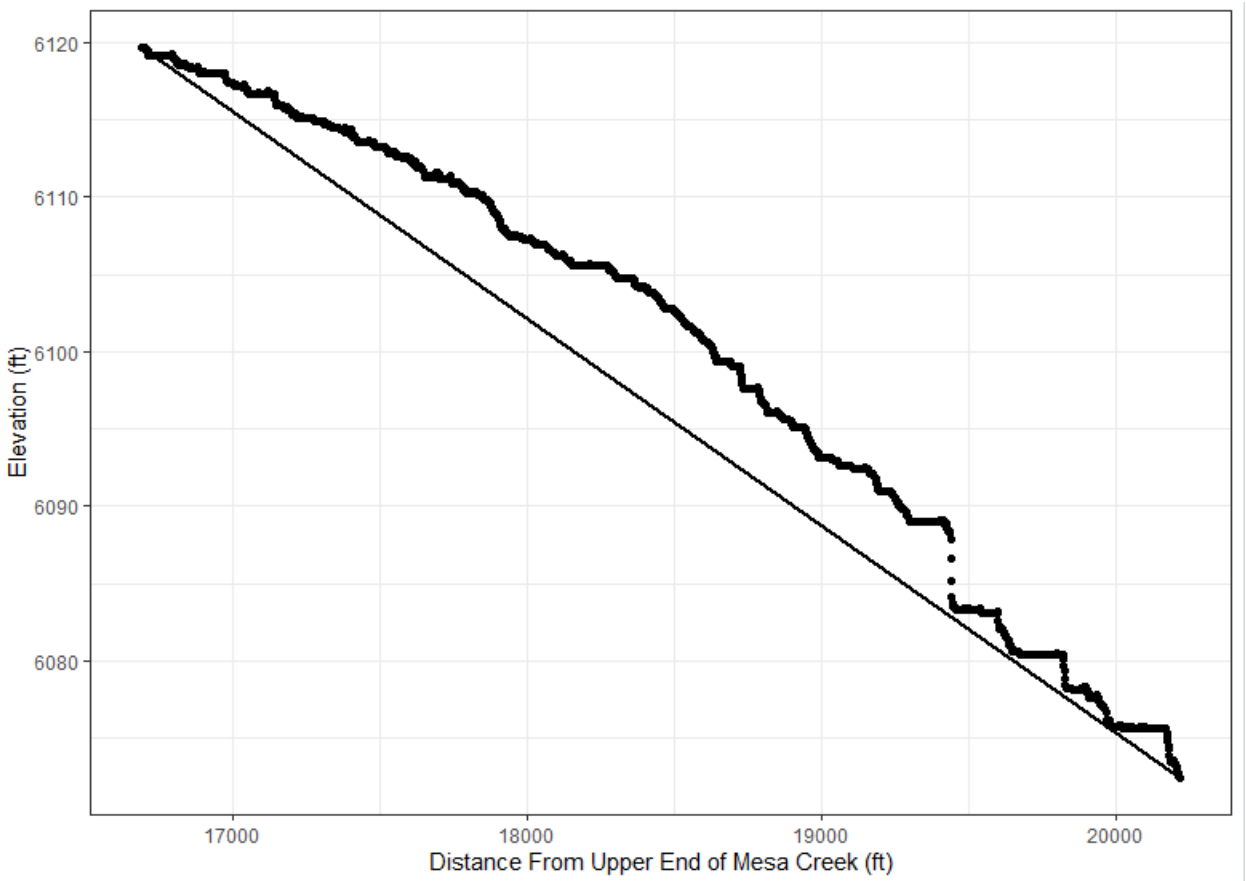

Figure 29. Longitudinal profile of Mesa Creek within the study area. Thick points represent the profile extracted from the 2-ft lidar, while the thinner black line is the average slope through the study area.

3.4.2.4. Channel profile

Within the study area, Mesa Creek has a convex profile with distinct steps in the last 500 feet (*Figure 29*). Streams in equilibrium tend to display concave-up profiles, where the slopes are steepest at the upstream end of the stream and gradually decrease further downstream (Howard, 1988). That Mesa Creek displays a convex profile through the study area implies the reach is in disequilibrium and does not currently have a stable long profile. Channel convexities can be associated with active tectonics, lithologic boundaries, or aggradation. There is no evidence that faulting is directly impacting Mesa Creek, and bedrock maps show no change in lithology within the study area (*Figure 2*). Thus, the convexity is likely due to sediment aggradation on the order of ~5 feet (*Figure 29*). This is apparent in field observations near Channel ID 3 and 4, where the base of drowned cottonwood trees is buried by 2-3 feet of sediment (*Figure 12*). Knickpoints at the downstream end of the study area, notably the large drop at 19,500 feet distance in *Figure 29*, are likely a result of upstream-propagating erosion into the aggradation zone; as knickpoints propagate upstream, they return the profile to a convex upward form. However, in doing so, these knickpoints also create erosion and adjust channel dynamics, as seen in the reach B5c that is entrenched and has much lower grain size and depth complexity.

3.4.3 Summary

Channel complexity metrics reflect the potential for habitat, biodiversity, and geomorphic diversity; higher complexity is associated with a healthier ecosystem. Channel width complexity increases in the downstream direction, as expected, but in the downstream half is highly influenced by a large ponded region surrounding Channel ID 7. Ponding here is caused by woody debris jams just upstream of a knickzone. Vegetation is also associated with increasingly complex channel geometries, as indicated by the variability in depth along a cross section. Channels with a strong vegetation influence have significantly higher CVD with a median of 0.33 compared to the weakly influenced channels with a median of 0.05. Vegetation also exerts a moderate control on the bedload complexity, with higher vegetation control resulting in a greater bedload complexity. Qualitatively, the longitudinal profile indicates aggradation in the central part of Mesa Creek with incision and erosion progressing upstream. Knickpoints from upstream-propagating erosion are associated with Rosgen reach boundaries and often controlled by vegetation, as discussed in Section 3.1.2.

Overall, greater channel complexity and thus healthier ecosystems in Mesa Creek are associated with highly vegetated areas, as well as with downed vegetation in the form of woody debris that creates spatial and temporal width complexity.

3.5 Hydrologic Modeling

In addition to field observations, we performed hydraulic modeling of Mesa Creek in order to observe the responses of the creek to approximate and hypothetical hydrologic conditions that represent current and former flow regimes. The HEC-RAS software employed for this work allows us to input modern geometry and rainfall events and outputs flow inundation and shear stress, among other variables. We use the shear stress to estimate transported grain size, and validate our model results against field data. This section of the report broadens our ability to investigate the influence of urbanizing headwaters on the hydraulics in Mesa Creek by adjusting baseflow, precipitation, and land cover conditions.

3.5.1 Methods

The Hydrologic Engineering Center's River Analysis System (HEC-RAS) is an integrated hydraulic modeling software. It can be used to compute one dimensional steady flow water surfaces and simulate one dimensional and/or two-dimensional unsteady flow regimes, among other components of river analysis. All of the analysis components HEC-RAS is capable of running use common geometric data and hydraulic computation routines which can be visualized using the extensive spatial data integration and mapping tool, HEC-RAS Mapper.

We first developed a common HEC-RAS terrain geometry for Mesa Creek. The terrain of the watershed is based on 2-foot lidar (https://coloradohazardmapping.com/LidarDownload) that was imported into RAS Mapper to provide elevation data throughout the study area. Two land cover rasters were then overlaid on this terrain: (1) soils data from the U.S. Geological Survey (USGS) with assigned saturation metrics, and (2) impervious land-cover from the National Land Cover Database (NLCD). A roughness coefficient (Manning's n) of 0.03 for channels and grasslands and 0.06 for floodplain brushlands was also assigned to

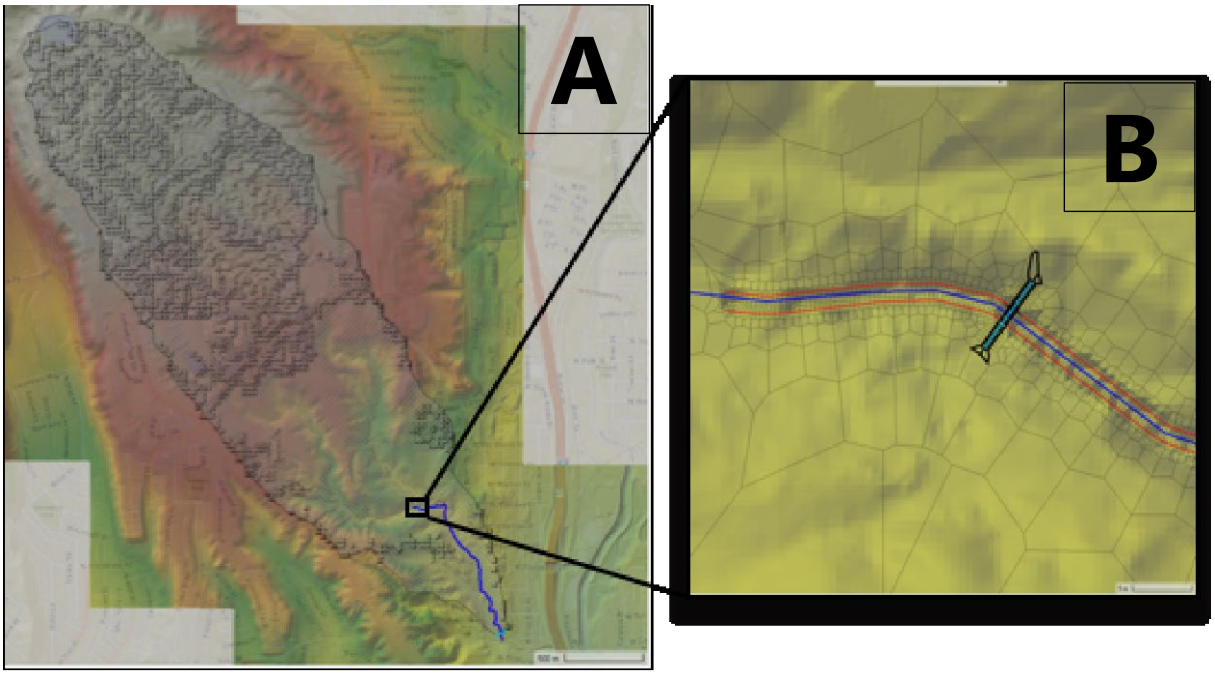

Figure 30. Hydraulic model geometry at the A) watershed scale (with elevation data, watershed boundary, and percent impervious land cover) and B) channel scale (with stream geometries, refined computational mesh, and input boundary condition).

the terrain. Then the geometry and boundaries of Mesa Creek were created in RAS Mapper (*Figure 30*). The channel geometry of Mesa Creek is too small to be captured with 2-foot lidar; therefore, the stream channel geometry was derived from the cross-sectional field data (*Figure 25*) (see Section 3.4 for locations of surveys and methods) and imbedded into the lidar terrain so that the modeling could use high-resolution channel elevation data. Bank lines were manually drawn along the left and right banks of Mesa Creek and a river centerline drawn that falls between either bank lines. This centerline is approximated in places due to the resolution of the lidar terrain. Once the river geometries were complete, cross sections perpendicular to the centerline were generated every 100 feet for use in later analysis.

The final step of setting up the geometry for HEC-RAS modeling was to create a computational mesh and boundary conditions. This mesh was generated at 100-meter intervals over the watershed and refined to a 0.67-meter grid along the Mesa Creek channel. Two boundary conditions were then defined: one at the model input and one at the output. The output boundary condition was drawn along the base of the watershed and allows hydraulic flow out of the downstream extent of Mesa Creek. The input boundary condition controls the modeled hydraulic inflow and lies perpendicular to the channel centerline (*Figure 30*). This boundary condition acted as the source of hydrographs during the model runs.

Six models were run with HEC-RAS for this study with three adjustable variables: precipitation data, base flow, and imperviousness (*Table 5*). First, two historical precipitation events from the nearby Camp Creek precipitation station (USGS 07103703) from July 2021 and August 2018 were used as inputs for the HEC-

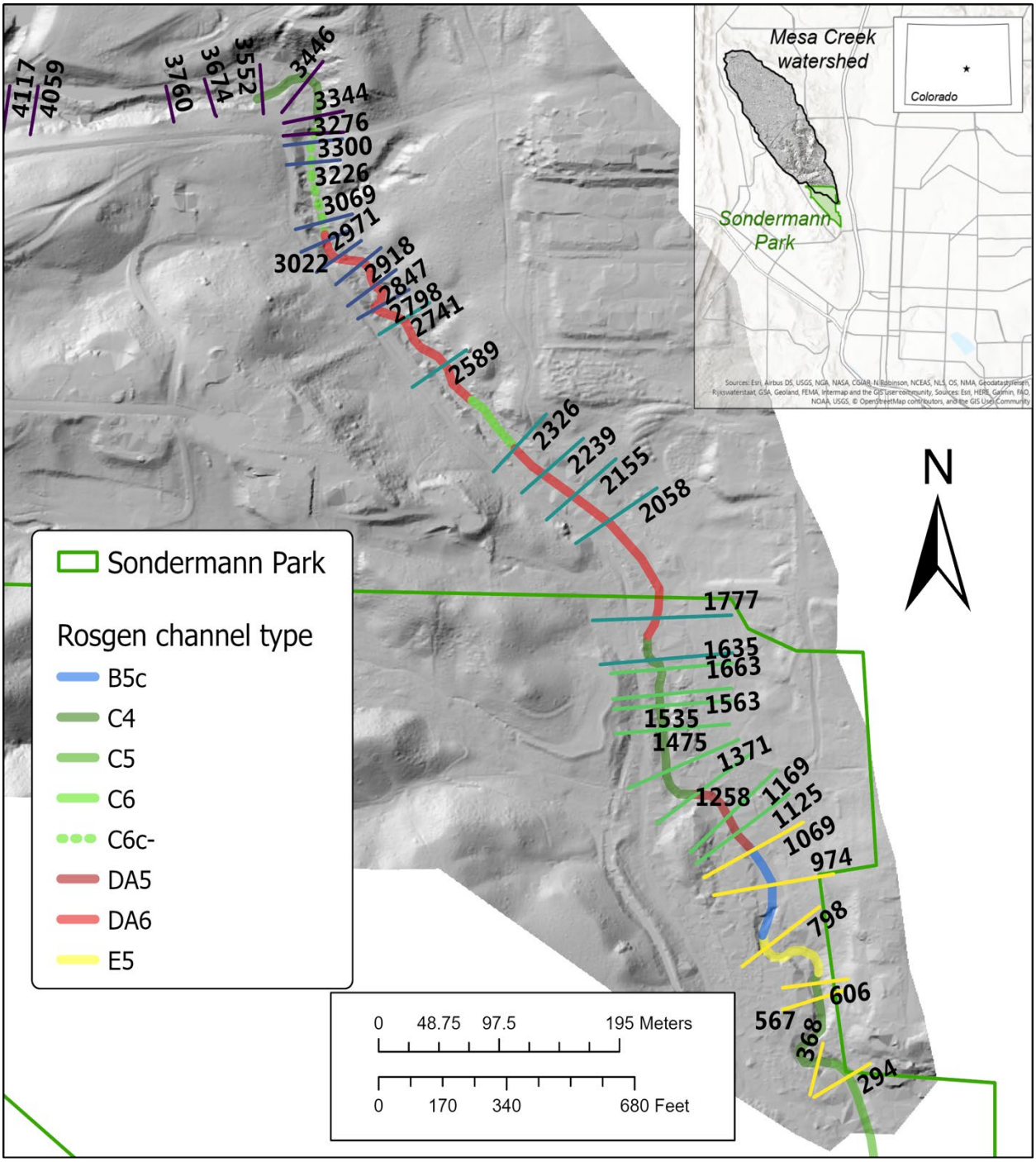

Figure 31. HEC-RAS cross-section station numbers for Mesa Creek, which correspond to upstream distance in feet. Cross sections are colored by upstream distance, and Rosgen reaches shown for reference.

Table 5. Description of hydrologic conditions used during HEC-RAS modeling

Simulation number	Precipitation Data (from USGS station 07103703)	Baseflow (cms)	% Impervious (*from NLCD, 2011)
1	July 15-16, 2021 (9.6mm/7hr)	0.003	0%
2	July 15-16, 2021 (9.6mm/7hr)	0.001	0%
3	July 15-16, 2021 (9.6mm/7hr)	0.003	0-100%*
4	August 21-22, 2018 (11.2mm/26hr)	0.003	0%
5	August 21-22, 2018 (11.2mm/26hr)	0.001	0%
6	August 21-22, 2018 (11.2mm/26hr)	0.003	0-100%*

RAS models. The amount of rainfall from both precipitation events is consistent with the magnitude of local 2-year storms (U.S. Geological Survey, 2016). The difference is that it took 26 hours for 11.2 mm of rain to fall in August 2018, whereas the July 2021 had a higher intensity with 9.6 mm precipitation in only 7 hours. The precipitation data was used to run rain-on-grid models from which stream flow hydrographs were obtained along the input boundary condition line. A second simulation was then run without rainfall but using the resultant hydrographs as inputs at the upstream boundary condition. This method lowers computation expense while allowing us to simulate 2-D unsteady flow conditions. We assume no significant discharge inputs between the start and end of our simulation; this assumption is justified by the lack of flowing tributaries within our study reach.

We also varied the baseflow discharge to simulate the effects of increased irrigation post-Kissing Camels construction (*Table 5*). Simulations used either 0.003 or 0.001 cubic meters per second (cms). Current baseflow is approximately 0.003 cms (0.1 cfs) based on measurements made during field work in the Mesa Creek watershed. The lower 0.001 cms (0.03 cfs) condition is an estimated value meant to approximate pre-irrigation stream flow conditions.

Finally, two conditions of imperviousness were examined in this study. One was a watershed with no impervious surfaces that simulations a pre-development landscape. The other condition uses the contemporary percent impervious land cover data from the NLCD. The three factors were combined so that we could compare, for each precipitation intensity: A) the effect of irrigation and increased baseflow on flooding extent and power, and B) the effect of urbanization and increased imperviousness on flooding extent and power.

For each simulation, top width and shear stress are extracted. The top width is the maximum width of wetted channel and represents the extent of flood inundation during storm events. The shear stress is used to calculate grain size mobility using the equation:

$$D_{50} = \frac{\tau}{0.0495 * (\rho_s - \rho_w) * g}$$

Where D_{50} is the median grain size transported, τ is the shear stress in N/m^2, ρ_s and ρ_w are the density of sediment and water in kg/m^3, respectively, and g is gravitational acceleration in m/s^2. The transportable grain size can then be compared to the field study results of modern bedload sediment size.

3.5.2. Results

3.5.2.1. Sediment transport and erosion

The grain size mobility calculated from the HEC-RAS simulations aligns with the modern bedload measured in Mesa Creek. The modeled D50 sediment size ranges from 0.012 to 205 mm, with median values of 0.075 to 0.29 mm. Extremely high calculated grain sizes result from surges in the HEC-RAS model in which water flow is irregular and does not approximate reality. This is due to the small channel size of Mesa Creek combined with heavy vegetation cover in the lidar that creates an irregular topography. When these values over 25 mm and values of 0 mm are removed, the average D50 grain size for each model run is 1 to 3.4 mm.

The median grain size (D50) measured in the field ranges from 0.25 to 2.75 mm (*Figure 16*). These field values are similar to the average D50 grain sizes in the HEC-RAS simulations, though slightly higher than the median D50 values. The modern channel, however, also includes grains transported in larger flows; the HEC-RAS modeling only used storm events analogous to the 50% annual exceedance probability (AEP) floods, yet it is entirely conceivable that the larger sediment grains observed in the bedload of Mesa Creek have been transported and deposited by less frequent, but more powerful, precipitation events. However, that the field and calculated D50 values are similar in range and order of magnitude suggests that the modelling is replicating shear stress conditions for Mesa Creek, and gives us more confidence that model results reflect field conditions.

The distinct precipitation, baseflow and impervious surface conditions are compared in *Figure 32*. Although slightly less total rain fell in the simulated July 2021 rainstorm, the higher intensity storm had greater transport potential due to flashier flows, resulting in a broader range of grain sizes transported than in the lower intensity August 2018 event. This indicates that flashier precipitation transports larger grain sizes in Sondermann Park via Mesa Creek. Similarly, when the baseflow is contrasted, a higher baseflow transports a wider range of grain sizes than the lower baseflow conditions. It is clear from these results that higher baseflow, in this case caused by increased irrigation of the Mesa Creek watershed, increases grain size mobility and has likely increased grain size in the channel. This finding is consistent with our field data that shows coarser grain sizes in the modern channel than in the historic terraces.

Finally, simulations in which impervious surfaces were varied to modern levels had no difference when compared to pre-urbanization simulations. This suggests that either: 1) our model set up was incorrect; 2) native soil type is already highly impervious and so an increase in impervious surfaces does not change runoff; and/or 3) the system of drains and retention basins is effectively trapping and releasing runoff. Since the impervious surfaces showed no change in shear stress simulations, we do not discuss it in the next section regarding flow inundation.

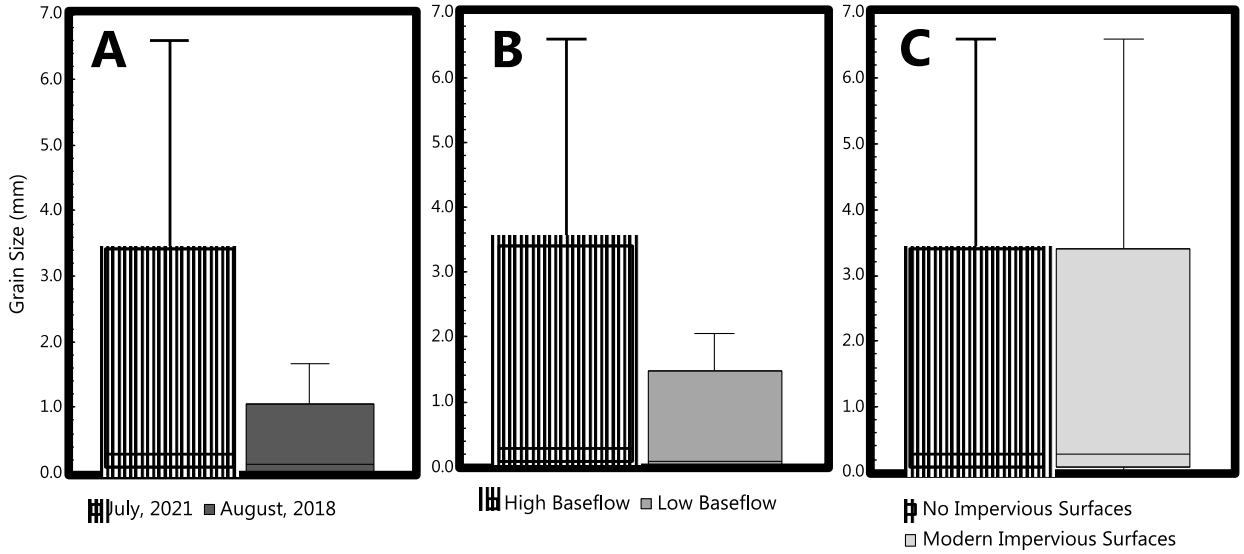

Figure 32. Comparison of grain size distributions for four simulations. A) high intensity versus low intensity storms using high baseflow and low impervious surface; B) high versus low baseflow using the July 2021 storm and low impervious surface; and C) modern versus historic impervious surfaces using the July 2021 storm and high baseflow. Shading and color is unique to each model run in

Table 5.

3.5.2.2. Flow inundation

Potential flood inundation is measured by the maximum water surface top width at each HEC-RAS cross section (*Figure 33*). Cross sections with low maximum top widths can be considered resistant to inundation while those with large top widths are points at which Mesa Creek may be prone to flooding. Top width varies from 3 cm up to 2.7 meters and increases downstream with a moderate but significant (p-value < 0.05) correlation of 0.22 to 0.26 for all simulations except the high intensity and high baseflow simulation. This latter simulation has a lower correlation of 0.12 and poor significance (p-value = 0.26). Since discharge remains constant, the increase in top width downstream reflects geometric changes that promote ponding and lateral inundation. The weak correlation of 0.26 or lower for all simulations with distance suggests high spatial variability in inundation. Particularly, there are reaches that uniformly experience low inundation such as at 2750 meters upstream, and others that uniformly experience high inundation such as that at 1500 meters upstream. Flood extent in these reaches is relatively insensitive to baseflow or storm intensity, and are reaches where consistent inundation can be expected. These may be good target reaches for infrastructure such as bridges and picnic benches. In contrast, several reaches have inundation levels that vary by meters depending on the baseflow and storm intensity; these may be reaches where set-back floodplains and undeveloped areas are necessary.

The high and low intensity storms don't have systematic and consistent trends. We expected that high intensity storms would be flashier and cause wider inundation patterns. However, 60% of our cross sections have simulated top widths within 0.2 m of each other for the six simulations, and 87.5% are within 0.5 meters. This suggests that flood inundation through the study area is relatively similar despite storm intensity and base flow. However, one cross section at 800 meters has a range of 1.56 meters in inundation width; this cross section will thus be more dynamic and less stable.

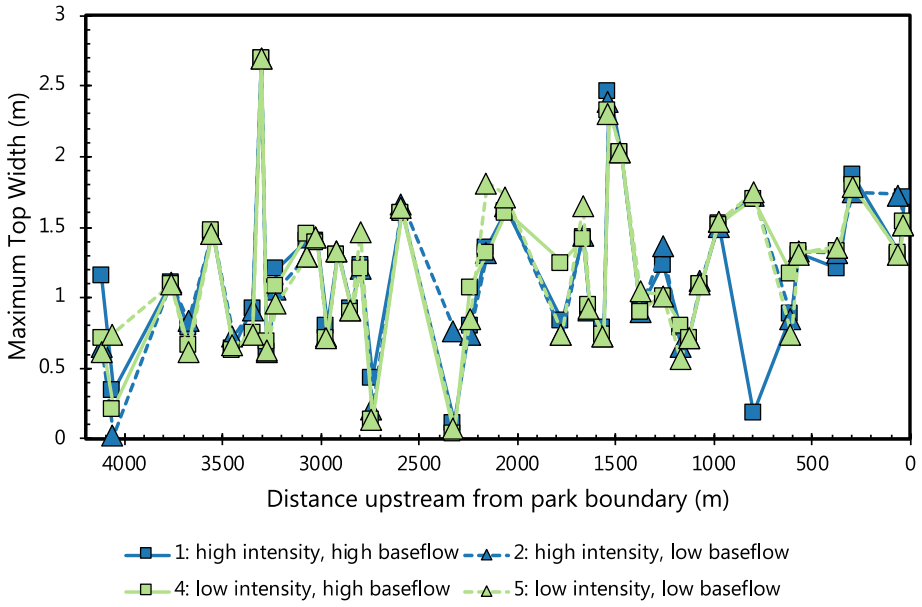

Figure 33. Maximum top width at HEC-RAS cross sections along Mesa Creek with the higher intensity event (July 2021) in blue compared to lower intensity event (August 2018) in green. Square symbols correspond to high baseflow, triangles to low baseflow. Distances correspond to the cross-section labels in Figure 31 and are distance upstream of park boundary in feet.

The effect of a high or low baseflow appears to be greater for the flashy storms. In the low intensity storm simulation, top width for high and low baseflows are relatively similar, with a maximum difference of 0.5 meters at the 4000 m cross section and a mean difference of 0.1 ± 0.15 meters. In contrast, the high intensity simulations display much wider variability between high and low baseflow with a maximum difference of 1.54 meters and a mean of 0.13 ± 0.27 meters. As baseflow is altered mostly by increased irrigation of the headwaters, these results imply that the effect of irrigation on flood extent is greater in higher intensity storms, but is fairly low in moderate to low intensity storms. However, top width in the high intensity simulations was not consistently higher in either high or low baseflow, suggesting the effect of baseflow on inundation in high intensity storms is very site-specific.

3.5.3 Summary

Despite the small size of Mesa Creek, 2-D HEC-RAS models reproduced shear stresses that match observed grain sizes, providing support for the model results. When flashier rain events with higher baseflow are modelled, larger grain sizes and range in sizes are predicted, which matches intuition. This also confirms field observations that show an increase in grain sizes after upstream irrigation began. Flood extents in the model are highly variable across the study area; some reaches have consistent flood extents for any baseflow and storm intensity, while other reaches are highly sensitive. Sensitivity increases with storm flashiness and that effect is amplified when higher baseflow is simulated. No changes were noted when the impervious surfaces were altered in the model. This suggests that irrigation effects rather than impervious surface development has a stronger influence on Mesa Creek, and that irrigation has increased the variability in flood extents and channel disturbance.

4. Limitations

This study was conducted over the 3.5 weeks of Block 6 with HEC-RAS modelling in additional 3.5 weeks in Block 7. The limited time constraints meant that we could not sample more sites or do >3 week monitoring of Mesa Creek. The major limitations are:

FIELD SAMPLING

- Sediment sampling was limited by the season; ice and snow cover prevented sediment sampling on many channel banks. Ideally, every in-stream sediment sample should be paired with a floodplain or terrace sample but this was not possible in March.
- On-going construction of the Centennial Boulevard extension and future construction of homes at the north end of the study area represent large disturbances to the system. Future work on sediment size characteristics and channel incision/aggradation during and after these construction projects will be needed.
- Our vegetation studies and ecological observations were limited by our lack of knowledge of plants and animals. Leaf loss in winter also inhibited plant identification, which could help us understand the impact that native and non-native species have on geomorphic complexity.

HEC-RAS

- Low resolution land cover data does not allow for detailed flow calculations to be performed across the Mesa Creek watershed.
- Lidar resolution is not adequate for mapping the fine Mesa Creek channel geometry. The physical channel is too small in places to be mapped by lidar and can easily be obscured by vegetation or blend with the adjacent floodplain.
- Low discharge and precipitation rates in the Mesa Creek watershed do not work well with the terrain developed in HEC-RAS. Ponding occurs on the terrain which resulted in cyclical trickling and flooding. The hydrology and discharge of Mesa Creek are not great enough to maintain a constant flow state during HEC-RAS modeling.

5. Conclusions

Mesa Creek is an urbanizing watershed responding to an increase in baseflow caused by upstream irrigation and nonnative water inputs and an increase in impervious surfaces and surface-water drainage. Our investigation focused on the current geomorphic state of Mesa Creek and used historic aerial photos, sediment archives, and numerical modelling to investigate the impact of aforementioned development on vegetation, grain size, and flood extents. We found that:

- A variety of channel types are present at Mesa Creek that alternate between multiple and single channels and tend to have low entrenchment values. Spatial correlation between vegetation root control and in-stream debris indicates a strong vegetation control on channel type.
- Greater channel complexity is associated with stronger vegetation root control.
- Channel complexity has altered over time due to baseflow. The historic channel was wide and braided; it has since narrowed to a single thread channel with evidence of 2-5 feet of aggradation in the 20th century. Narrowing is coincident with development of dense vegetation, which provides channel complexity in the absence of dynamic braided channels.

- Modern channel sediment has a bimodal distribution that reflects dominant geology of Pikes Peak Granite and Pierre Shale.
- Historic grain sizes were smaller and indicate lower transport capacity in the past. The change in transport capacity can be caused by channel narrowing, lower slopes, and/or more water; all three changes are observed in historical records.
- Numerical modelling corroborates field observations that grain size has increased due to a higher baseflow, and indicates that introduction of non-native water through irrigation has led to more unpredictable flooding patterns in Mesa Creek.

6. Works cited

Booth, D.B., Fischenich, C.J., 2015. A channel evolution model to guide sustainable urban stream restoration. Area 47, 408–421. https://doi.org/10.1111/area.12180

Booth, D.B., Roy, A.H., Smith, B., Capps, K.A., 2016. Global perspectives on the urban stream syndrome. Freshw. Sci. 35, 412–420. https://doi.org/10.1086/684940

Bunte, K., Abt, S.R., 2001. Sampling Surface and Subsurface Particle-size Distributions in Wadable Gravel- and Cobble-bed Streams for Analyses in Sediment Transport, Hydraulics, and Streambed Monitoring. U.S. Department of Agriculture, Forest Service, Rocky Mountain Research Station.

Chin, A., 2006. Urban transformation of river landscapes in a global context. Geomorphology, 37th Binghamton Geomorphology Symposium 79, 460–487. https://doi.org/10.1016/j.geomorph.2006.06.033

city-data, 2019. Old dump at the end of Cenetnnial (Colorado Springs, Black Forest: house, landscaping) - (CO) - City-Data Forum [WWW Document]. URL http://www.city-data.com/forum/colorado-springs/3071933-old-dump-end-cenetnnial.html (accessed 6.24.22).

Hawley, R.J., Bledsoe, B.P., Stein, E.D., Haines, B.E., 2012. Channel Evolution Model of Semiarid Stream Response to Urban-Induced Hydromodification1. JAWRA J. Am. Water Resour. Assoc. 48, 722–744. https://doi.org/10.1111/j.1752-1688.2012.00645.x

Howard, A.D., 1988. Equilibrium models in geomorphology, in: Modelling Geomorphological Systems. John Wiley & Sons, Ltd, pp. 49–72.

KRDO, 2019. Locals worried about an old landfill contaminating Mesa Creek. KRDO. URL https://krdo.com/news/2019/08/08/locals-worried-about-an-old-landfill-contaminating-mesa-creek/ (accessed 6.24.22).

Laub, B.G., Baker, D.W., Bledsoe, B.P., Palmer, M.A., 2012. Range of variability of channel complexity in urban, restored and forested reference streams. Freshw. Biol. 57, 1076–1095. https://doi.org/10.1111/j.1365-2427.2012.02763.x

Peel, M.C., Finlayson, B.L., McMahon, T.A., 2007. Updated world map of the Köppen-Geiger climate classification. Hydrol. Earth Syst. Sci. 11, 1633–1644. https://doi.org/10.5194/hess-11-1633-2007

Peters, S.E., Husson, J.M., Czaplewski, J., 2018. Macrostrat: A Platform for Geological Data Integration and Deep-Time Earth Crust Research. Geochem. Geophys. Geosystems 19, 1393–1409. https://doi.org/10.1029/2018GC007467

Rosgen, D.L., 1994. A classification of natural rivers. CATENA 22, 169–199. https://doi.org/10.1016/0341-8162(94)90001-9

Russell, K.L., Vietz, G.J., Fletcher, T.D., 2018. Urban catchment runoff increases bedload sediment yield and particle size in stream channels. Anthropocene 23, 53–66. https://doi.org/10.1016/j.ancene.2018.09.001

Scott, G.R., Cobban, W.A., 1965. Geologic and biostratigraphic map of the Pierre shale between Jarre Creek and Loveland, Colorado (No. I–439). https://doi.org/10.3133/i439

Soil Survey Staff, Natural Resources Conservation Service, United States Department of Agriculture, n.d. Web Soil Survey [WWW Document]. URL http://websoilsurvey.sc.egov.usda.gov/ (accessed 3.16.22).

Stinchcomb, G.E., Driese, S.G., Nordt, L.C., Allen, P.M., 2012a. A mid to late Holocene history of floodplain and terrace reworking along the middle Delaware River valley, USA. Geomorphology 169–170, 123–141. https://doi.org/10.1016/j.geomorph.2012.04.018

Stinchcomb, G.E., Driese, S.G., Nordt, L.C., Allen, P.M., 2012b. A mid to late Holocene history of floodplain and terrace reworking along the middle Delaware River valley, USA. Geomorphology 169–170, 123–141. https://doi.org/10.1016/j.geomorph.2012.04.018

U.S. Geological Survey, 2016. The StreamStats program for Colorado [WWW Document]. URL http://water.usgs.gov/osw/streamstats/colorado.html (accessed 3.1.22).

Van Meter, K., Thompson, S.E., Basu, N.B., 2016. Human Impacts on Stream Hydrology and Water Quality, in: Jones, J.B., Stanley, E.H. (Eds.), Stream Ecosystems in a Changing Environment. Academic Press, Boston, pp. 441–490. https://doi.org/10.1016/B978-0-12-405890-3.00011-7
White, J., Wait, T.C., 2003. Map of Potential Areas of Landslide Susceptibility in Colorado Springs, El Paso County, Colorado.